NASA CONTRACTOR REPORT

NASA CR-1041

NASA CR-1041

COATING SELECTION PROGRAM

Theory

by Frederick A. Costello, Thomas P. Harper, and Barbara Aston

Prepared by
GENERAL ELECTRIC COMPANY
Philadelphia, Pa.

for

NATIONAL AERONAUTICS AND SPACE ADMINISTRATION • WASHINGTON, D. C. • APRIL 1968

DISCLAIMER NOTICE

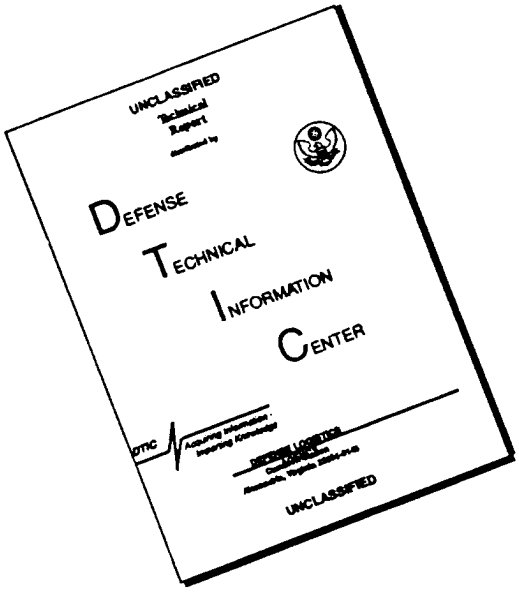

THIS DOCUMENT IS BEST QUALITY AVAILABLE. THE COPY FURNISHED TO DTIC CONTAINED A SIGNIFICANT NUMBER OF PAGES WHICH DO NOT REPRODUCE LEGIBLY.

NASA CR-1041

COATING SELECTION PROGRAM

Theory

By Frederick A. Costello, Thomas P. Harper, and Barbara Aston

Issued by Originator as Document No. 65SD526

Prepared under Contract No. NASw-960 by
GENERAL ELECTRIC CO.
Philadelphia, Pa.

for

NATIONAL AERONAUTICS AND SPACE ADMINISTRATION

For sale by the Clearinghouse for Federal Scientific and Technical Information
Springfield, Virginia 22151 — CFSTI price $3.00

19960607 090

RECEIVED NEW REPORT, PAGE 9-9 IS

BLANK

JULY 2, 1996

ABSTRACT

A rational and direct method has been developed for selecting the optical coating pattern for the external surface of a spacecraft, such that the spacecraft temperatures are as close as possible to the midpoint of their preselected ranges. The temperature control is maintained passively by radiation and conduction, using no active control devices. The complete range in mission environments is considered in the optimization procedure.

The selection technique has been programmed for use on the GE 600 Series, IBM 7094, or any other computer that uses the standard IBM Fortran IV system.

FORWORD

This document is a three-part final report on the Coating Selection Program. Part I describes the theory and basis for selection of: (1) the iteration scheme used to solve the heat balance equations; and (2) the optimization scheme. Part II describes the computer program, including the details of each subroutine and the details of input and output. Part II therefore includes the user's manual. Part III presents the Program Listing. Parts I, II and III have been revised (Revision A) under a contract extension to incorporate descriptions of the first two month's usage, as well as a new Program Listing with improvements as found advisable during these two months.

The work reported herein was sponsored by the National Aeronautics and Space Administration and was monitored by Mr. Conrad Mook, of NASA-Headquarters, and Mr. Robert Kidwell, Jr., of NASA's Goddard Space Flight Center.

The chief contributors to the work reported were Mr. Frederick A. Costello, Engineer, who developed the techniques, Mr. Thomas P. Harper, Analyst, who converted the techniques to computer form, both of the Re-entry Systems Department's Thermodynamics Technology Component, and Miss Barbara Aston, Programmer-Analyst, from the Spacecraft Department, who programmed the technique for computer usage.

CONTENTS

CONTENTS (Cont'd)

ILLUSTRATIONS

TABLES

1.0 INTRODUCTION

The use of optical coatings to control the temperatures of satellites has been exploited since the first successful orbital flight in 1958 (Explorer). Since then, coating materials have been developed to the point where coatings are available[1] that give any desired emittance value between 0.1 and 0.9 for any desired absorptance value between 0.1 and 0.9. What has lagged, however, is the development of a systematic approach to selecting coating patterns for the external surface of the vehicle, such that the satellite temperatures are passively maintained as close as possible to the optimum temperature. It was in response to this developmental need that the present work was undertaken. The work discussed in this report constitutes a generalization of the work performed by Costello, Harper, and Cline[2].

For the uninitiated, an example may prove useful in illustrating the effect of proper coating-pattern selection. Figure 1 shows the environmental conditions for a typical satellite, as well as the optimum coating pattern and resulting temperatures. It is seen that using two different coatings rather than one narrows the temperature excursions from $\pm 7F^{O}$ to $\pm 5F^{O}$ from the desired $70^{O}F$. This result is not as dramatic as those obtained for more complicated shapes. Further improvement is still possible, but the point is adequately illustrated.

The solution to simple coating selection problems, as shown in Figure 1, is indeed difficult, but the complexity and difficulty increase rapidly as the number of surfaces increases and as the number of critical components increases. For realistic satellite designs, it is usually necessary to include the entire conduction and radiation heat transfer networks; consequently, the selection process is obscured by the various interactions and by the number of degrees of freedom (twice the number of external surfaces). Such complexity demands the use of a high-speed computational device. From the beginning, then, the present work has been directed toward the development of an IBM 7094 digital-computer program that would assist the designer in the coating selection process.

In the following sections, the coating-selection problem is formulated in mathematically precise terms. The mathematical development of the minimization scheme is presented in Sections 3.0, 4.0 and 5.0. Applications are considered in Section 6.0. The work is summarized in Section 7.0 and future areas for research are cited in Section 8.0.

It should be recognized that operating experience is important to the efficient usage of a computer program. The present program has, as all programs do, a variety of input constants that affect such things as iteration procedures and optimization sequences. An extention to the original contract enabled a study of the input constants. The study was conducted by analyzing several vehicle designs, three of which are shown in section 6. The operating experience obtained from the study along with recommended procedures for use of the program is summarized in the User's Manual. It is felt that the study, permitted by the contract extention, has enhanced significantly the benefits of the program.

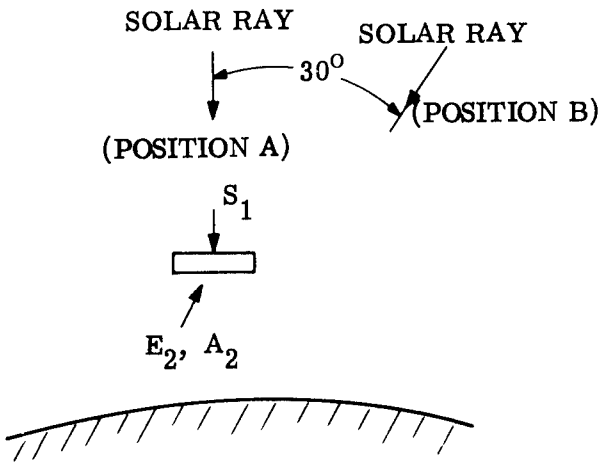

Orbit	Heat Fluxes			
	Side 1	Side 2		
Solar Angle	Solar Flux	Earth Flux	Albedo Flux	
0^o	140.0	70.0	50.5	BTU / Hr-Ft^2
30^o	121.0	70.0	43.5	

Coating Limit
$0.1 \leq \alpha \leq 0.9$
$0.1 \leq \epsilon \leq 0.9$

$T = 70^oF$ is desired

Single Coating

$$(140 + 50.5)\,\alpha + (70)\,\epsilon = 2\,\epsilon\,\sigma\,T^4$$

$$(121 + 43.5)\,\alpha + (70)\,\epsilon = 2\,\epsilon\,\sigma\,T^4$$

Best Solution

α	ϵ	T
0.9	0.8	$63\text{-}77^oF$

Double Coating

$$140\,\alpha_1 + 50.5\,\alpha_2 + 70\,\epsilon_2 = (\epsilon_1 + \epsilon_2)\,\sigma\,T^4$$

$$121\,\alpha_1 + 43.5\,\alpha_2 + 70\,\epsilon_2 = (\epsilon_1 + \epsilon_2)\,\sigma\,T^4$$

Best Solution

α_1	α_2	ϵ_1	ϵ_2	T
0.4	0.5	0.345	0.5	$65\text{-}75^oF$

Figure 1. Example of Two-Coating Advantages

2.0 PROBLEM STATEMENT

As intimated in the Introduction, the purpose of the present work was to develop a computer program that would determine the optical coating pattern that minimizes temperature excursions from some preselected temperatures for all possible environmental conditions. More precisely, we define the excursion parameter, β_{ik} as

$$\beta_{ik} \equiv \max \left[\left(\frac{T_{ik} - T_{iU}}{T_{iU} - T_{iL}} \right); \left(\frac{T_{iL} - T_{ik}}{T_{iU} - T_{iL}} \right) \right] \tag{2.1}$$

Where T_{ik} is the temperature of the i^{th} network element (node) in the k^{th} orbit, and T_{iU} and T_{iL} are the upper and lower allowable temperature limits of the i^{th} node. We wish to find the surface coating properties of infra-red emittance, ϵ, and solar absorptance, α, such that

$$\beta \equiv \max_{i,k} \beta_{ik} = \min \tag{2.2}$$

subject to the constraints that α and ϵ are within a preselected allowable range.

From the above definitions, it is obvious that (-1/2) is the absolute minimum value of β_{ik} and that $\beta \leq 0$ implies that all nodes are within their allowable temperature limits.

Physically, the above formulation implies that the coating system is selected to minimize the temperature excursion of the node that is furthest from the midpoint of its allowable temperature range.

Other Possible Criteria

The above criterion, Equation (2.2), was selected from a number of alternates, the most interesting of which were

$$\gamma_1 \equiv \sum_{i,k} (\beta_{ik})^2 = \min \tag{2.3}$$

$$\gamma_2 \equiv \sum_{i} (C_i \alpha_i + \alpha_i \epsilon_i) = \min \tag{2.4}$$

subject to the additional constraints $\beta_{ik} \leq 0$

Equation (2.3) was the most convenient from a mathematical viewpoint, but γ_1 could be a minimum when one temperature was so far out of range as to make the solution ridiculous.

Equation (2.4) resembles a linear programming formulation and is physically the most satisfying. However, the equations are significantly non-linear, and the optimum may lie at large distances from the vertices of the restraint volume.

Time-Dependent Solutions

Inherent in the above problem statement is the assumption that the critical temperature can be adequately calculated using time-averaged environmental heat fluxes. This is an important and restrictive assumption, complicated by the fact that the time constants of each node are different and vary non-linearly with the node temperature. In Section 8.0, further study is recommended in this area. In the meantime, however, the average-flux procedure should serve as a useful guide in selecting the optimum coating pattern. The average-flux analysis can be made quite accurate if the emittance is kept low and/or the node heat capacities kept high, so that all the time constants are significantly greater than, say, the orbit period.

Development of Solution

The solution to Equation (2.2) can be conveniently, but not completely, divided into two steps: (1) solving for the T_{ik}'s, given a set of α's and ϵ's; and (2) selecting new values of α and ϵ to reduce β. The first problem is discussed in Section 3.0; the second, in Sections 4.0 and 5.0.

3.0 SOLVING THE HEAT-BALANCE EQUATIONS

The node temperatures are governed by the heat-balance equations:

$$\underbrace{\sum_j K_{ij}\,(T_{ik} - T_{jk})}_{\text{conduction interchange}} + \underbrace{\sum_j \sigma\, R_{ij}\,(T_{ik}^4 - T_{jk}^4)}_{\text{radiation interchange}} = \tag{3.1}$$

$$= \underbrace{\alpha_i\,(K_{Si}\,S_{ik}}_{\substack{\text{incident}\\ \text{solar}\\ \text{flux}}} + \underbrace{K_{Ai}\,A_{ik})}_{\substack{\text{incident}\\ \text{albedo}\\ \text{flux}}} + \underbrace{\epsilon_i\,(K_{Ei}\,E_{ik}}_{\substack{\text{incident}\\ \text{earth}\\ \text{flux}}} - \underbrace{a_i\,\sigma\,T_{ik}^4)}_{\text{re-emission}} + \underbrace{K_{Q_i}\,Q_{ik}}_{\substack{\text{internal}\\ \text{heat}\\ \text{generation}}}$$

$$\underbrace{\qquad\qquad}_{\text{absorbed solar energy}} \qquad \underbrace{\qquad\qquad}_{\text{net absorbed IR energy}}$$

where

i, j = node numbers = $1, 2, \ldots, N + S$

k = orbit, or time-interval, number = $1, 2, \ldots, q$

and where the nomenclature is described in Appendix D (Section 9.0).

Equation (3.1) can be written in the more compact form

$$\sum_j \bar{A}_{ij}\,T_j + \sum_j M_{ij}\,T_j^4 = \alpha_i\,S_i + \epsilon_i\,E_i - \epsilon_i\,a_i\,\sigma\,T_i^4 + Q_i \tag{3.2}$$

$$i = 1, 2, \ldots, N$$

where for convenience we have dropped the k (orbit number) subscript. In discussing solutions to Equation (3.2), it is frequently necessary to examine the symmetrically linearized form:

$$\sum_j L_{ij}\,T_j = C_i \tag{3.3}$$

where

$$L_{ij} = \begin{cases} -K_{ij} - \sigma\,R_{ij}\,(\tilde{T}_i + \tilde{T}_j)\,(\tilde{T}^2_i + \tilde{T}^2_j) & i \neq j \\ -\sum\limits_{\substack{j=1 \\ j \neq i}}^{N+S} L_{ij} + 4\,a_i\,\epsilon_i\,\sigma\,\tilde{T}_i^3 & i = j \end{cases} \tag{3.4}$$

$$C_i = \alpha_i (K_{Si} S_i + K_{Ai} A_i) + \epsilon_i (K_{Ei} E_i + 3 a_i \sigma \tilde{T}_i^4) K_{Q_i} Q_i$$

where once again k has been dropped.

Many methods for solving the linear system, Equation (3.3), have been devised. A convenient and up-to-date summary is given by Fox[3]. These methods have been adapted to the present set of equations and the speeds of convergence compared. In addition, two new matrix-inversion methods have been examined. In the following paragraphs, each method is described. All methods make use of the residual vector, r_i:

$$r_i^{(n)} = \left[\alpha_i S_i + \epsilon_i E_i - \epsilon_i a_i \sigma T_i^4 + Q_i - \sum_j \bar{A}_{ij} T_j^{(n)} - \sum_j M_{ij} (T_j^{(n)})^4\right] \tag{3.5}$$

When the exact solution is obtained, $r_i = 0$ for all values of "i".

Gauss-Seidel Methods

Applied to the linear system, Equation (3.3), the extrapolated Gauss-Seidel method gives:

$$T_i' = \frac{C_i - \sum_{j<i} L_{ij} T_j^{(n+1)} - \sum_{j>i} L_{ij} T_j^{(n)}}{L_{ii}}$$

$$T_i^{(n+1)} = \frac{1}{\alpha_n} T_i' + \frac{\alpha_n - 1}{\alpha_n} T_i^{(n)}$$

In terms of the residual vector, this may be written

$$T_i^{(n+1)} = T_i^{(n)} + \frac{r_i^{(n)} + \sum_{j<i} L_{ij} (T_j^{(n)} - T_j^{(n+1)})}{\alpha_n L_{ii}} \tag{3.6}$$

(Symmetrically Linearized Gauss-Seidel)

The factor α_n is the extrapolation ($\alpha_n < 1$) or interpolation ($\alpha_n > 1$) factor.

Equation (3.6) was used directly for the present non-linear case, with the residual vector defined by Equation (3.5).

In the non-stationary iteration process, α_n is governed by the equation

$$\alpha_n = 1 - \frac{T^{(n+1)} - T^{(n)}}{T^{(n)} - T^{(n-1)}}$$

However, from the experience of Kaplan[4], it is necessary to restrict α_n between 1/2 and 1 to obtain convergence for the heat-balance equations. For the present case, α_n was taken as 1.0, a constant.

Some saving in computation can be realized if the linearization process applied to Equation(3.2) takes a Taylor-series form:

$$\sum_j \bar{A}_{ij} T_j + \sum_j M_{ij} T_j^4 \doteq \sum_j \left[(\bar{A}_{ij} + 4M_{ij} \tilde{T}_j^3) T_j - 3 M_{ij} \tilde{T}_j^4 \right]$$

In this case, the iteration formula becomes

$$T_i^{(n+1)} = T_i^{(n)} + \frac{r_i^{(n)} - \sum_{j<i} \left[\bar{A}_{ij} + 4M_{ij} \tilde{T}_i^3 \right] \left[T_j^{(n+1)} - T_j^{(n)} \right]}{\left[\bar{A}_{ii} + 4 M_{ii} \tilde{T}_i^3 \right]} \qquad (3.7)$$

Maximum Rate of Descent

Applied to Equation (3.3), the maximum rate of descent method described by Fox[3] gives:

$$T_i^{(n+1)} = T_i^{(n)} + \left[\frac{\sum_j r_j^{(n)} r_j^{(n)}}{\sum_{i,j} L_{ij} r_i^{(n)} r_j^{(n)}} \right] r_i^{(n)} \qquad (3.8)$$

This was carried over directly, using Equation (3.5) to calculate r_j.

Conjugate Gradient Method

Fox gives for the linear system

$$T_i^{(n+1)} = T_i^{(n)} + \left[\frac{\sum_j w_j^{(n)} r_j^{(n)}}{\sum_{i,j} L_{ij} w_i^{(n)} w_j^{(n)}} \right] w_i^{(n)} \qquad (3.9)$$

where

$$w_i^{(n)} = \begin{cases} r_i^{(n)} & n = 0 \\ r_i^{(n)} - \left[\dfrac{\sum_{i,j} L_{ij} r_i^{(n)} w_j^{(n-1)}}{\sum_{i,j} L_{ij} w_i^{(n-1)} w_j^{(n-1)}} \right] w_i^{(n-1)} & n \geq 1 \end{cases}$$

Once again, using Equation (3.5) to define r_j, Equation (3.9) can be used in the non-linear case.

Newton-Raphson Method

The Newton-Raphson method uses Equation (3.5) directly, taking

$$r_i^{(n+1)} = r_i^{(n)} + \sum_j \left(\frac{\partial r_i}{\partial T_j}\right)^{(n)} \left[T_j^{(n+1)} - T_j^{(n)}\right]$$

Setting $r_i^{(n+1)}$ equal to zero gives

$$T_i^{(n+1)} = T_i^{(n)} - \sum_j \bar{N}_{ij}^{(n)} r_j^{(n)}$$

where $\left\{\bar{N}_{ij}\right\}$ is the inverse of the matrix $\left(\frac{\partial r_i}{\partial T_j}\right)^{(n)}$ where

$$\left(\frac{\partial r_i}{\partial T_j}\right)^{(n)} = \begin{cases} -\bar{A}_{ij} - 4 M_{ij} T_j^3 & i \neq j \\ -4 \epsilon_i a_i \sigma T_i^3 - \bar{A}_{ij} - 4 M_{ij} T_j^3 & i = j \end{cases}$$

This method requires a matrix inversion at each iteration and was found slower than the matrix-inversion method described next.

One way of alleviating the difficulty of inverting a matrix each time is to use an approximate inverse in the form

$$\begin{aligned} (\tilde{E} + \epsilon)^{-1} &= \left[\tilde{E}\left(I + \tilde{E}^{-1}\epsilon\right)\right]^{-1} \\ &= \left[I - \tilde{E}^{-1}\epsilon\right]^{-1} \tilde{E}^{-1} \\ &= \left(I - \tilde{E}^{-1}\epsilon\right)\tilde{E}^{-1} \end{aligned}$$

Then the expression for $T^{(n+1)}$ becomes, for $\tilde{E}_{ij} = \left(\frac{\partial r_i}{\partial T_j}\right) T_j = T_j^{(o)}$ and $\tilde{N} = \tilde{E}^{-1}$

$$T_i^{(n+1)} = T_i^{(n)} - \sum_j \tilde{N}_{ij} r_j^{(n)} + \sum_{j,k,l} \tilde{N}_{ij} \epsilon_{jk}^{(n)} \tilde{N}_{kl} r_l^{(n)} \quad \text{(Expanded Inverse)}$$

where

$$\epsilon_{ij}^{(n)} \begin{cases} -4 M_{ij} \left[(T_j^{(n)})^3 - (T_j^{(o)})^3\right] & i \neq j \\ -4\left[\epsilon_i^{(o)} a_i \sigma + M_{ij}\right] \cdot \left[(T_j^{(n)})^3 - (T_j^{(o)})^3\right] & i = j \end{cases}$$

Matrix Inversion Methods

A direct Matrix Inversion method of solving Equation (3.2) can be obtained simply by writing:

$$T_i^{(n+1)} = \left\{\bar{A}'_{ij}\right\}^{-1} \left\{ X_j T_j^{(n)} + \alpha_j S_j + \epsilon_j E_j - \epsilon_j a_j \sigma (T_j^{(n)})^4 + Q_j - \sum_k M_{jk} (T_k^{(n)})^4 \right\} \qquad (3.10)$$

where $\bar{A}'_{ij}$ differs from $\bar{A}_{ij}$ in that a convergence factor, X_i, has been added, according to the convergence criteria of Appendix B (Section 9.0). Note that Equation (3.10) converges quite rapidly when the radiation terms are small.

Using the residual vector, Equation (3.10) can be written in the form

$$T_i^{(n+1)} = T_i^{(n)} + \sum_j J'_{ij} r_j^{(n)} \qquad \text{(Direct Matrix Inversion)} \qquad (3.11)$$

where

$$\left\{J'_{ij}\right\} = \left\{\bar{A}'_{ij}\right\}^{-1}$$

which is evaluated once per solution.

One improvement to Equation (3.11) can be obtained by writing Equation (3.2) in the form

$$\bar{A}''_{ij} = \begin{cases} \bar{A}_{ij} + M_{ij}\left[T_i^{(o)} + T_j^{(o)}\right] \cdot \left[(T_i^{(o)})^2 + (T_j^{(o)})^2\right] \equiv \bar{A}_{ij} + \bar{M}_{ij} & i \neq j \\ -\sum_{j \neq i} \bar{A}''_{ij} + 4\epsilon_i^{(o)} \sigma a_i (T_i^{(o)})^3 + X_i \equiv \bar{A}_{ii} + \bar{M}_{ii} & i = j \end{cases}$$

and

$$\sum_j (\bar{A}_{ij} T_j + M_{ij} T_j^4 + \bar{M}_{ij} T_j^{(o)}) = \alpha_i S_i + \epsilon_i E_i - \epsilon_i \sigma a_i T_i^4 + Q_i + \sum_j \bar{M}_{ij} T_j^{(o)}$$

Then

$$T_i^{(n+1)} = \sum_j J''_{ij} \left[\alpha_j S_j + \epsilon_j E_j - \epsilon_j \sigma a_j (T_j^{(n)})^4 + Q_j + \sum_k \bar{M}_{jk} T_k^{(o)} - \sum_k M_{jk} (T_k^{(n)})^4 \right]$$

In terms of the residual vector

$$T_i^{(n+1)} = T_i^{(n)} + \sum_j J''_{ij} r_j^{(n)} \qquad \text{(Linearized Matrix Inversion) (3.12)}$$

J''_{ij} is evaluated once per solution.

Comparison of Methods

It is beyond the scope of this development program to develop the system of theorems required to compare the rates of convergence of the above methods of solving the heat-balance equations. Such a task is rendered difficult by the heterogeneous character of the iteration schemes. However, it is practical and important to evaluate the schemes numerically for typical satellite-type heat-balance equations. The methods are compared in Tables I and II.

There are several parameters that must be defined before the significance of the following numerical comparisons can be understood. Convergence is assumed to be completed if

$$\left| T_i^{(n+1)} - T_i^{(n)} \right| \leq DT \qquad i = 1, 2, \ldots, N$$

and

$$\left| r_i^{(n+1)} - r_i^{(n)} \right| \leq DR \qquad i = 1, 2, \ldots, N$$

In addition, those methods that use $\tilde{T}$, the linearizing temperature, update $\tilde{T}$ (i.e., let $\tilde{T} = T^{(n+1)}$ every time

$$\left| T_i^{(n+1)} - T_i^{(n)} \right| \leq DTR \qquad i = 1, 2, \ldots, N$$

Those methods using the convergence parameter, X, calculate the value of X using T_{MAX} and/or T_{SOL}.

TABLE I. SOLUTION TIMES FOR ITERATION SCHEMES $\left(\frac{\text{Millisec}}{(\text{Nodes})^{1.8}(\Delta T)^{0.4}}\right)$

Iteration Scheme	PROBLEM A	B	C
1. Direct Matrix Inversion	2.2	1.0	1.77
2. Linearized Matrix Inversion	1.8	1.1	1.27
3. Expanded Inverse	4.2	2.0	3.32
4. Linearized Gauss-Seidel	1.3	1.3	1.79
5. Symmetric Gauss-Seidel	1.8	1.7	2.63
6. MRD	2.7	2.7	3.19
7. Conjugate Gradient	1.6	1.2	1.42

NOTES

1. Problems Used Were:

   A. Pure Radiation ($h_r A \approx 1.0$ BTU/hr^{o}F, between adjacent nose)

   B. Pure conduction, except external surfaces which used pure radiation ($h_r A \approx 1.0$)

   C. Combined conduction/radiation; $h_r A \approx kA/x = 1.0$

   In all cases, 8, 16, and 64 node problems were considered. The geometry was a cube broken into equally sized cubes. The 8 node case used a 2 x 2 x 2 configuration; the 16, a 2 x 2 x 4; and the 64, a 4 x 4 x 4.

2. In general, DTR = DR = DT = 1.0 for the above cases. A 20% to 30% improvement was made in all methods but (1) and (2) by setting DTR = 0.0; that is, by not correcting the original linearization.

3. Methods 1, 2, and 3 require specification of T_{MAX} to assure convergence. The correlated time is good for $T_{MAX} \leq 1.3\ T_{SOL}$. A 20% increase in running time was experienced for $T_{MAX} = 1.5\ T_{SOL}$.

4. See Table II for actual running times and additional notes.

TABLE II. TIMING DATA FOR ITERATION SCHEMES

Problem	Nodes	ΔT (%)	Iteration Scheme (Times In $\frac{\text{Millisec}}{(\text{Nodes})^{1.8}(\Delta T)^{0.4}}$) 1	2	3	4	5	6	7
A	8	2.6	1.68	1.40	3.08	1.13	1.40	2.52	1.68
	16	2.4	1.61	1.28	3.37	1.21	1.77	2.67	1.53
	64	2.4	2.34	1.58	4.77	1.63	2.32	3.08	1.73
	8	15.6	1.45	1.18	2.89	0.92	1.18	1.05	1.32
	16	15.6	1.55	1.13	3.06	0.95	1.10	1.02	1.36
	64	15.6	2.25	1.63	4.56	1.45	1.70	1.19	1.55
B	8	2.4	1.12	.84	1.96	1.12	1.40	2.50	1.12
	16	2.4	.563	.723	1.45	1.12	1.69	2.56	1.12
	64	2.4	.482	.633	1.49	1.61	2.31	3.07	1.30
	8	15.6	.66	.79	1.58	0.92	1.05	1.32	1.05
	16	15.6	.416	.68	1.36	1.02	1.32	1.29	1.02
	64	15.6	.446	.66	1.5	1.36	1.83	1.47	1.15
C	8	2.4	1.68	1.40	3.08	1.68	2.24	3.48	1.40
	16	2.4	1.69	1.29	2.98	1.77	2.81	3.70	1.37
	64	2.4	2.19	1.41	4.24	2.42	4.13	4.70	1.47
	8	5.9	1.56	1.17	2.92	1.56	2.14	3.30	1.36
	16	5.9	1.50	1.17	2.90	1.56	2.40	3.24	1.28
	64	5.9	2.17	1.40	4.39	3.24	3.36	4.46	1.48
	8	15.6	1.58	1.18	2.76	1.32	1.72	1.45	1.45
	16	15.6	1.44	1.10	2.87	1.51	2.04	1.36	1.36
	64	15.6	2.13	1.39	3.96	2.05	2.84	1.53	1.53
D	8	15.6	.526	.789	1.32	4.48(1)	6.97(1)	4.21(1)	1.58
	16	15.6	.378	.642	1.28	6.65(2)	12.3(2)	8.69(2)	2.23
	64	15.6	.375	.673	1.39	7.63(2)	1.91(3)	15.2(2)	2.15(1)

NOTES:

1. For these runs, DT = 1.0 and DR = 0.5, but the converged solutions were 3 to 7°F in error.

2. For these runs, DT = 1.0 and DR = 0.5, but the runs were terminated for being unsuccessful after 100 iterations. Solutions are normally obtained in 10-20 iterations.

3. For this run, DT = DR = 1.0, but the converged solution was about 80°F in error.

4. ΔT is the change (in %) in equilibrium temperature, based on the initial temperature in °R, from the initial temperature to the exact final temperature (T_{SOL}).

5. The geometry used was a cube broken into equally sized cubes.

Examination of Tables I and II reveals that Method (2) is the fastest in nearly every case. One notable exception is the conduction dominated case (B), where Method (1) was faster. The reason for this is that (2) used too conservative a stability factor for these particular cases. If the normal values had been used (see Appendix B), Method (2) would have shown the approximately 20% improvement over Method (1) that is evident in the other cases analyzed.

One other case was studied that is not reported on the tables. This was a 67-node model of an ablative heat shield for a satellite/re-entry vehicle. For this problem, due to the peculiarities of the conduction matrix, $\overline{A}_{ij}$, only Methods (1) and (2) converged, the times correlating well with those shown on the tables. The other methods were no more than 1% of the way toward a solution after 100 iterations, indicating that their convergence times would be a factor of one thousand greater than the times indicated on Tables I and II.

The choice of methods, therefore, is clearly in favor of Method (2).

4.0 GEOMETRY OF THE β SURFACES

Of paramount importance in the development of any optimization scheme is foreknowledge of the geometry of the criterion surface. For example, if there is more than one minimum point, a method must be devised for first finding one minimum, then search for the second, and so on, to determine which point is the absolute minimum. In the following paragraphs, unimodality and other properties of the β-surface are examined.

Monotonic β_{ik}

The first important characteristic of β is that it is composed of segments of monotonic surfaces. That it is composed of segments of surfaces can be seen from the definition of β (see Equation 2.2). That β_{ik} is composed of two monotonic branches can be seen as follows:

The heat-balance equation can be written:

$$\sum_j \bar{A}_{ij} T_j + \sum_j M_{ij} T_j^4 = \alpha_i (K_{Si} S_i + K_{Ai} A_i) + \epsilon_i (K_{Ei} E_i - \sigma a_i T_i^4) + K_{Qi} Q_i \tag{4.1}$$

This equation can be linearized in T^4 according to the scheme

$$\sum_j \bar{A}_{ij} T_j = \sum_{j \neq i} \bar{A}_{ij} (T_j - T_i) + (\bar{A}_{ii} + \sum_{j \neq i} \bar{A}_{ij}) T_i$$

$$T_j - T_i \doteq \frac{T_j^4 - T_i^4}{(T_j + \tilde{T}_i)(T_j^2 + \tilde{T}_i^2)}$$

$$T_i \doteq \tilde{T}_i + \frac{T_i^4 - \tilde{T}_i^4}{4\tilde{T}_i^3} = \frac{3}{4}\tilde{T}_i + \frac{1}{4}\frac{T_i^4}{\tilde{T}^3}$$

Then Equation (4.1) becomes

$$\sum_{j=1}^{N} N_{ij} T_j^4 = \alpha_i (K_{Si} S_i + K_{Ai} A_i) + \epsilon_i (K_{Ei} E_i - \sigma a_i T_i^4) + K_{Qi} Q_i - \frac{3}{4}(\bar{A}_{ii} + \sum_{j \neq i} \bar{A}_{ij}) \tilde{T}_i + \\ - \sum_{j=N+1}^{N+S} M_{ij} T_j^4 - \frac{3}{4} \sum_{j=N+1}^{N+S} \bar{A}_{ij} T_j \tag{4.2}$$

where

$$N_{ij} = \begin{cases} M_{ij} + \bar{A}_{ij} (\tilde{T}_i + \tilde{T}_j)^{-1} (\tilde{T}_i^2 + \tilde{T}_j^2)^{-1} & i \neq j \\ -\sum_{i \neq j} N_{ij} + \frac{1}{4} \frac{1}{\tilde{T}_i^3} (\tilde{A}_{ii} + \sum_{i \neq j} A_{ij}) & i = j \end{cases} \tag{4.3}$$

Note that since $N_{ij} \leq 0$ for $i \neq j$ and $N_{ii} = -\sum_{j \neq i} N_{ij}$,

$$\left\{N_{ij}\right\}^{-1} \geq 0 \tag{4.4}$$

This property of $\left\{N_{ij}\right\}^{-1}$ holds regardless of the value of the $\tilde{T}_i$'s, since $\tilde{T}_i \geq 0$.

Equation (4.2) carries on the right-hand side one term involving $\tilde{T}_i$. This term vanishes if (a) there is no conduction, or (b) there are no constant-temperature nodes to which heat is conducted.

Equation (4.2) gives

$$\sum_{j=1}^{N} N_{ij} \frac{\partial T_j^4}{\partial \epsilon_\ell} = \delta_{i\ell} (K_{Ei} E_i - \sigma a_i T_i^4) - \epsilon_i \sigma a_i \frac{\partial T_i^4}{\partial \epsilon_\ell} \tag{4.5}$$

$$\sum_{j=1}^{N} N_{ij} \frac{\partial T_j^4}{\partial \alpha_\ell} = \delta_{i\ell} (K_{Si} S_i + K_{Ai} A_i) - \epsilon_i \sigma a_i \frac{\partial T_i^4}{\partial \alpha_\ell} \tag{4.6}$$

$$\sum_{j=1}^{N} N_{ij} T_j^4 = \alpha_i (K_{Si} S_i + K_{Ai} A_i) + \epsilon_i (K_{Ei} E_i - \sigma a_i T_i^4) + K_{Qi} Q_i - \frac{3}{4} \sum_{j=N+1}^{N+S} \bar{A}_{ij} (T_j - \tilde{T}_i) + \\ - \sum_{j=N+1}^{N+S} M_{ij} T_j^4 \tag{4.7}$$

Since $\left\{N_{ij} + \epsilon_i \delta_{ij}\right\}$ has the same properties of $\left\{N_{ij}\right\}$,

$$\left\{N_{ij} + \epsilon_i \delta_{ij}\right\}^{-1} \equiv \left\{P_{ij}\right\} \geq 0$$

Therefore, from Equation (4. 6), T^4 is monotonically increasing with α_ℓ. To determine how T_i^4 varies with ϵ_ℓ, define

$$Y_i = \sigma a_i T_i^4 - K_{Ei} E_i$$

Then

$$\frac{\partial Y_i}{\partial \epsilon_\ell} = \sigma a_i \frac{\partial T_i^4}{\partial \epsilon_\ell} \tag{4. 8}$$

and

$$\sum_j \left(\frac{N_{ij}}{\sigma a_j} + \epsilon_i \delta_{ij} \right) \frac{\partial Y_j}{\partial \epsilon_\ell} = \delta_{i\ell} Y_i \tag{4. 9}$$

$$\sum_j \left(\frac{N_{ij}}{\sigma a_j} + \epsilon_i \delta_{ij} \right) Y_j = \left[\alpha_i (K_{Si} S_i + K_{Ai} A_i) - \sum_{j=1}^{N} \frac{N_{ij}}{\sigma a_j} E_j + K_{Qi} Q_i - \frac{3}{4} \sum_{j=N+1}^{N+S} \bar{A}_{ij} (T_j - \tilde{T}_i) + \right.$$

$$\left. - \sum_{j=N+1}^{N+S} M_{ij} T_j^4 \right] \equiv (RHS)_i \tag{4. 10}$$

Therefore, from Equation (4. 9)

$$\frac{\partial Y_k}{\partial \epsilon_\ell} = P_{k\ell} Y_\ell$$

or

$$\frac{\partial Y_k}{\partial \epsilon_\ell} = \sum_{i=1}^{N} P_{k\ell} P_{\ell i} (RHS)_i \tag{4. 11a}$$

Since $\{P_{ij}\} \geq 0$, Equation (4. 11) indicates that Y_k increases or decreases with ϵ_ℓ depending on the signs of the right-hand-sides.

If $(K_{Si} S_i + K_{Ai} A_i) \neq 0$ for all values of "i", then Equation (4. 6) shows that no T_j^4 - surface has a horizontal point. If $(K_{Si} S_i + K_{Ai} A_i) = 0$ for all "i", Equation (4. 11a) must be examined, along with the definition of $(RHS)_i$, Equation (4. 10).

$$\frac{\partial Y_k}{\partial \epsilon_\ell} = \sum_{i=1}^{N} P_{k\ell} P_{\ell i} \left[Q_i - \sum_{j=1}^{N} N_{ij} \frac{E_j}{\sigma a_j} - \frac{3}{4} \sum_{j=N+1}^{N+S} \bar{A}_{ij} (T_j - \tilde{T}_i) - \sum_{j=N+1}^{N+S} M_{ij} T_j^4 \right]$$

(4.11b)

Within the accuracy of the linearization, the expression for $(RHS)_i$ is a constant, independent of the values of α and ϵ. Its sign, therefore, will not change over a given Y_k (or T_k^4) surface. Since $\{P_{k\ell}\}$ is positive, $\frac{\partial Y_k}{\partial \epsilon_\ell}$ also will not change sign on the Y_k surface.

The conclusion to be drawn from the above is that the Y_k, and therefore T_k^4 and T_k (see Equation (4.8)), have no extremes inside the boundaries of any given Y_k surface.

A similar analysis linearizing T^4 into T leads to the same conclusion. Trying to solve the non-linear case directly is frustrated by the lack of an explicit expression for Y_k in Equation (4.9).

Consider next a composite surface, β, defined by

$$\beta = \max_{i,k} \beta_{ik}$$

where

$$\beta_{ik} = \max \left[\left(\frac{\sigma T_{ik}^4 - \sigma T_{iD}^4}{\sigma T_{iU}^4 - \sigma T_{iL}^4} \right); \left(\frac{\sigma T_{iD}^4 - \sigma T_{ik}^4}{\sigma T_{iU}^4 - \sigma T_{iL}^4} \right) \right]$$

$$= \max \left[\left(\frac{(Y_{ik} - E_{ik})/a_i - \sigma T_{iD}^4}{\sigma T_{iU}^4 - \sigma T_{iL}^4} \right); \left(\frac{\sigma T_{iD}^4 - (Y_{ik} - E_{ik})/a_i}{\sigma T_{iU}^4 - \sigma T_{iL}^4} \right) \right]$$

$$= \max \left[(C_1 Y_{ik} - C_2) ; (C_2 - C_1 Y_{ik}) \right]$$

Define

$$\beta_{ikU} = C_1 Y_{ik} - C_2$$

$$\beta_{ikL} = C_2 - C_1 Y_{ik}$$

Now the β_{ikL} and β_{ikU} have the same properties of the Y_k's analyzed above. Equations (4.6) and (4.11) imply that the minimum value of β must occur at the intersection of at least two β_{ik} surfaces.

Unimodality of β

The next objective is to show that the preceding properties lead to the conclusion that there can be only one relative minimum point. Suppose there were two, say β_1 and β_2. Then around each of these points

$$\delta\beta \geq 0 \tag{4.12}$$

Therefore there is a relative maximum, β_3, lying along a continuous but broken path following the axes between Points 1 and 2. Then around β_3

$$\delta\beta \leq 0 \tag{4.13}$$

Consider a line through Point 3 parallel to the x_i axis. A variation in β along the axis is designated $\delta\beta_i$. Now the condition (4.13) implies that

$$\beta(x_i + \delta x_i) = \beta(x_i) + \left(\frac{\partial\beta}{\partial x_i}\right)\left|\delta x_i\right|$$

$$\beta(x_i - \delta x_i) = \beta(x_i) - \left(\frac{\partial\beta}{\partial x_i}\right)\left|\delta x_i\right|$$

or

$$\delta\beta_i^+ = \left(\frac{\partial\beta}{\partial x_i}\right)^+\left|\delta x_i\right|$$

$$\delta\beta_i^- = -\left(\frac{\partial\beta}{\partial x_i}\right)^-\left|\delta x_i\right|$$

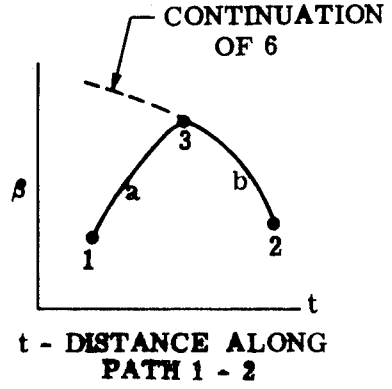

Although β is discontinuous at Point 3, the surfaces that intersect there are sections of infinite, continuous, and monotonic surfaces, so that

$$\left(\frac{\partial\beta}{\partial x_i}\right)^+ = \left(\frac{\partial\beta}{\partial x_i}\right)^-$$

Therefore, if $\delta\beta_i^+ > 0$, $\delta\beta_i^- < 0$, contradicting Equation(4.13). Therefore there cannot be two discrete minima. However, if $\delta\beta = 0$, there may be an infinite number of minima connected by a continuous path.

Concavity of β

A surface is simple or concave if for any two points on the β- surface, β_1, and β_2,

$$\beta\left[\lambda\,\bar{x}_1 + (1-\lambda)\,\bar{x}_2\right] \leq \lambda\,\beta\left[\bar{x}_1\right] + (1-\lambda)\,\beta\left[\bar{x}_2\right]$$

If we consider a line along the ϵ_i axis, Equation (4.11) shows that β_{ik} is either convex or concave. Therefore β has segments that are concave and other segments that are convex. β is therefore not strictly concave or convex.

Figure 2 shows a typical β_{ik} surface, from which the β surface is constructed. Figure 3 shows a typical map for a one-node/one-external-surface problem.

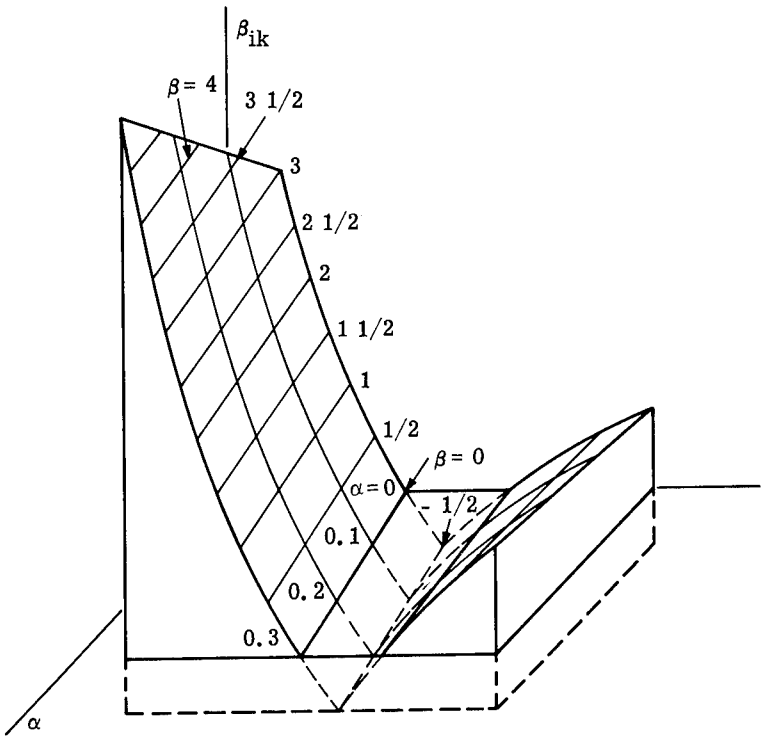

Figure 2. Section of a Typical β_{ik} Surface

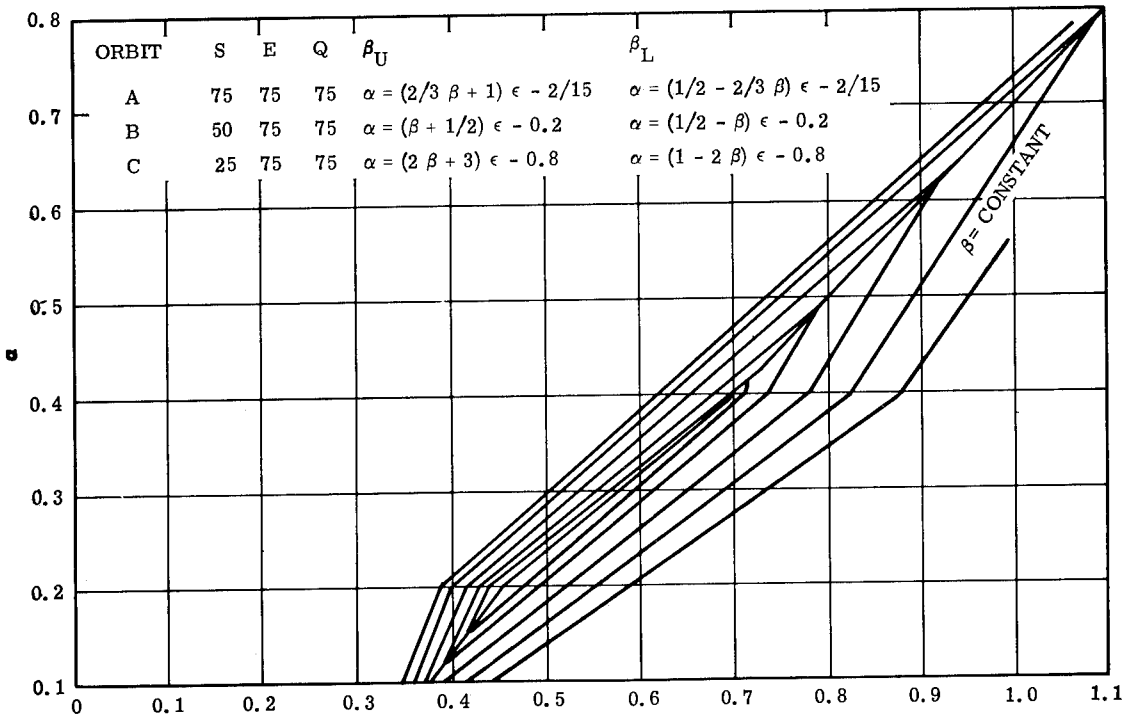

Figure 3. Map of β Surface for One-Node Case

5.0 OPTIMIZATION SCHEMES

Several optimization schemes were considered for use in the present program. These included:

(a) Linear Programming

(b) Pattern Search

(c) Miguel's Poor-Man's Ridge Follower

(d) Variational Methods

(e) Hill-climbing (Maximum Rate of Descent, or MRD)

Methods (b) and (c), which are described in Wilde's book: "Optimum Seeking Methods," can fail to find the minimum due to the extremely sharp ridges (discontinuous derivatives) characteristic of the β - surfaces.

Method (d), used in many trajectory optimization schemes, is frustrated by the fact that β has discontinuous derivatives. It is possible, however, to redefine β and consider the independent variables to be α_i, ϵ_i, and T_i, subject to the constraints

$$T_{iL} \leq T_i \leq T_{iU}$$

$$\alpha_{iL} \leq \alpha_i \leq \alpha_{iU}$$

$$\epsilon_{iL} \leq \epsilon_i \leq \epsilon_{iU}$$

This leads to a rapid solution if the solution satisfies these limits within the constraints of the heat balance equation.

The most severe disadvantage of the variational scheme is the number of computations required if the constraints cannot be met. For example, a three-node problem, each with independent values of α, ϵ, and T, has N = 9 independent variables. Considering both upper and lower bounds on the variables, the heat-balance equation must be solved S times, where

$$S = 2^{(N-1)} \sum_{j=1}^{N} \frac{N!}{(N-j)!\, j!}$$

$$= 2^8 \sum_{j=1}^{9} \frac{9!}{(9-j)!\, j!}$$

$$= 13180$$

In the MRD scheme, S is on the order of 100 to 200. Since most of the computation time is spent solving the heat-balance equation, the variational scheme need not be considered further.

Method (a), although quite powerful in linear problems, depends on the accuracy of linearization for nonlinear problems. It is anticipated, on the basis of past experience, that some of the external-surface temperatures will range from say $300^{\circ}R$ to $500^{\circ}R$ due to orbit-to-orbit changes in the relative position of the sun. Linearization, therefore appears dangerous. In addition, if there is no feasible solution, a rather extensive sensitivity analysis would be necessary to determine what must be done to obtain a feasible solution.

Suppose, however, that these objections were overcome. The linear-programming time per iteration would be on the order of

$$\text{Time } (\mu\text{sec}) = 1000\ p\ N^2 + 61\ N^3\ (1 + p) + 400\ p\ q\ r$$

$$+ \frac{(2\ rp + 2q)\ (2\ rp + 4q)^2 \times 10^3}{12}$$

where

N = number of nodes
p = number of orbits
q = number of external nodes
r = number of critical nodes

For reasonably sized problems, the last term dominates. In fact, one finds the time nearly proportional to $(rp)^3$. The following table gives some time estimates for q equal to 10.

r	p	Time (sec)
5	5	25
	10	130
10	5	200
	10	1060
20	5	1570
	10	8450
30	5	5300
	10	28500

For problems of this general size, MRD would take an estimated 3,600 seconds.

From the foregoing discussion, it may be concluded that the MRD approach appears most promising due to the highly non-linear character of the equations, the long running times for LP systems with no feasible solutions, and the comparable running times between LP and MRD for systems of common complexity and with feasible solutions. Hence, MRD was selected for the present program.

The MRD method is described in many texts[5]. It involves selecting a starting point (a set of α_i's and ϵ_i's) and calculating the criterion function (β) as well as

the values of $(\partial\beta/\partial\alpha_i)$ and $(\partial\beta/\partial\epsilon_i)$ at this point. Using the derivatives, the direction in which $\left(\frac{\partial\beta}{\partial s}\right)$ is a maximum can be determined where

$$(ds)^2 = \sum_j \left[(d\epsilon_j)^2 + (d\alpha_j)^2\right]$$

Then for a given (Δ s), $\Delta\beta$ will be a maximum, and β will decrease more than if any other direction had been used (provided Δs is small enough). Thus a step-by-step procedure is used to decrease β, where each step is taken in the local maximum-rate-of-descent direction.

MRD converges to the optimum very slowly when it encounters a sharp ridge, such as are characteristic of the β -surface defined by Equation (2.1). Several ridge-following techniques are described in the literature, but these are frustrated by the extreme sharpness of the present ridges. None use the ridges to assist in finding the solution. Therefore, a method called TREND was devised for the present problem.

In TREND, use is made of the fact that the β_{ik} surfaces are monotonic, so that when a ridge is crossed, say from Point 1 to Point 2, one of the subscripts of β_{ik} changes (or a switch from upper to lower bound occurs). If the ridge is immediately re-crossed to, say Point 3, this indicates that the points being studied lie in a valley. A vector extrapolation from Point 1 through Point 3 gives an improved value of β (see Appendix A). Figure 4 illustrates the process. The vector $\overline{P1,\ P3}$ is in the downward direction of the valley and indicates the trend of the valley. In many test cases, it has been found that TREND results in a time saving of 1.5:1 to 10:1 over the conventional MRD methods.

The logic diagram for the computer program developed in the present work, using the TREND procedures, is shown in Appendix C (Section 9.0).

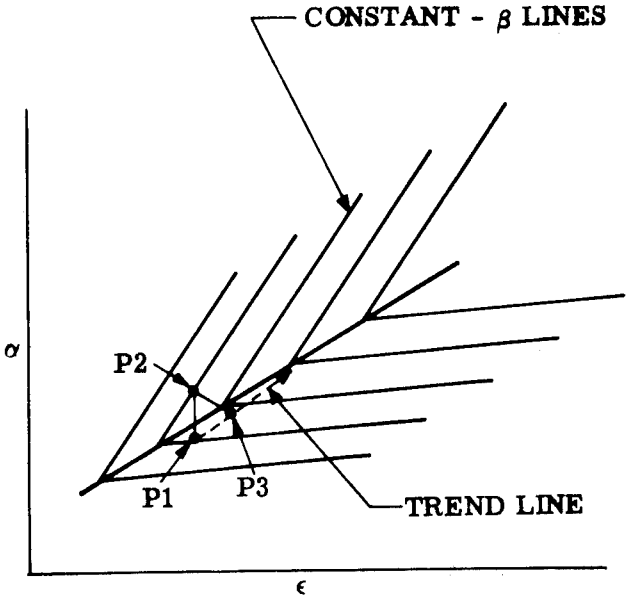

Figure 4. Illustration of TREND Method

6.0 APPLICATIONS

FICTITIOUS SATELLITE

As an example of the use of the foregoing theory, the problem of optimizing the coating pattern of a cylindrical, horizontally stabilized earth satellite will be considered. Figures 5 and 6 show the details of the satellite geometry, the orbits considered, and the arrangement of the coating patches.

Table III shows the heat fluxes (BTU/hr-ft^2) on each patch for the range in solar angles shown on Figure 6. These are the average heat fluxes over one orbit period.

The details of the input/output procedures and the actual computer program are shown in Section 5 of Part II of this final report. The results, however, are summarized on Table IV. The importance of the optimization process is obvious on examination of Table IV. Even for an optimized single-coating pattern, the temperature excursions from the desired mean are 50% greater than can be attained with the multi-patch coating.

NASA EPE-D

A second example was supplied by Mr. Robert Kidwell of NASA-GSFC. This was a mathematical model of the NASA EPE-D (Explorer XXVI) Satellite. The nodal breakdown is shown on Figure 7 and a photograph of the actual satellite is shown on Figure 8. The orbit of this satellite is such that the heat flux received from the earth is negligible. The significant parameter is the angle between the solar ray and the spin axis. In this case, instead of orbit number, the different sets of heat fluxes represent different angles between solar ray and spin axis.

The engineers at GSFC had had some experience with the temperature response of satellites of this configuration. These investigators undertook a trial-and-error procedure using considerable engineering judgement to select a suitable coating pattern for the EPE-D. Mr. Kidwell estimates that at least 4 weeks and 4 hours of computer time were required to achieve the desired results. Table V shows the temperature ranges attained, along with the allowable ranges. Only the critical nodes are shown on this table.

The challenge was to determine if the computer program could be used to improve on this design and the design procedure. The Coating Selection Program did devise two better coating patterns. The results of the one-week study are also summarized on Table V. A total of approximately 40 minutes of computer time was used. This shows that the program can reduce costs by a factor of four.

NASA IMP-C

A third example was again supplied by Mr. Robert Kidwell of NASA-GSFC. This was a mathematical model of the NASA IMP-C satellite. The nodal breakdown is shown in Figure 9, and a photograph of the actual satellite is shown in Figure 10. The Coating Selection Program devised a better coating pattern than the one devised by the engineers at GSFC. The study using the Coating Selection Program took one week and 50 minutes of computer time which also represents a significant gain over the original design procedure used at GSFC. The results are summarized in Table VI.

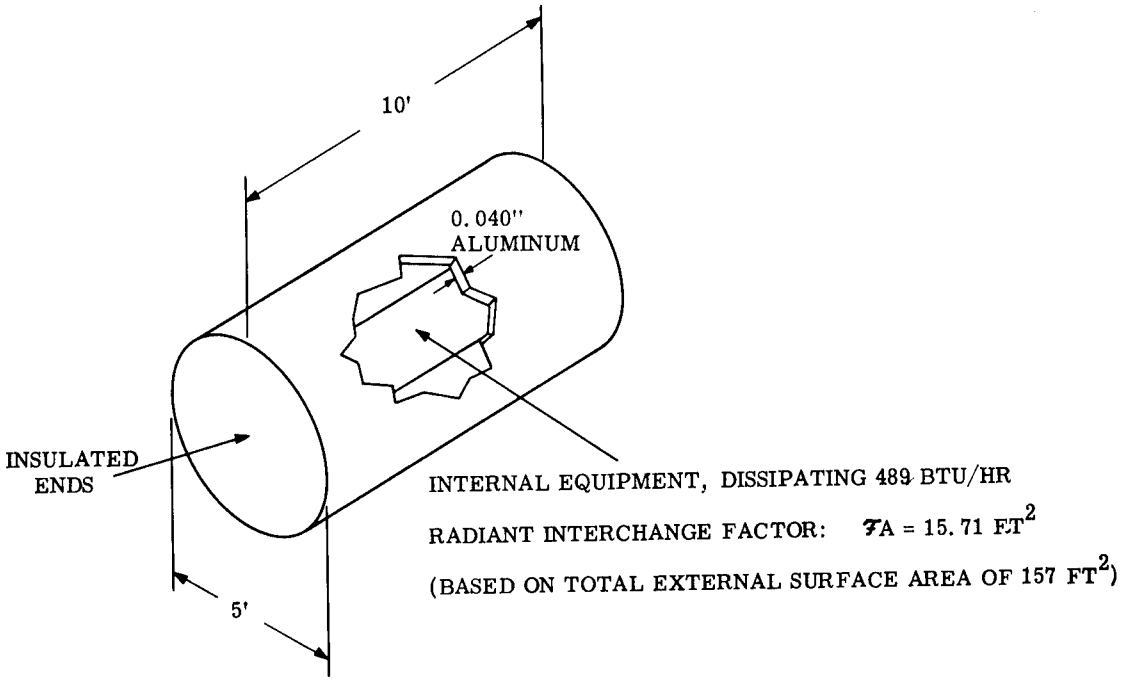

Figure 5. Vehicle Geometry

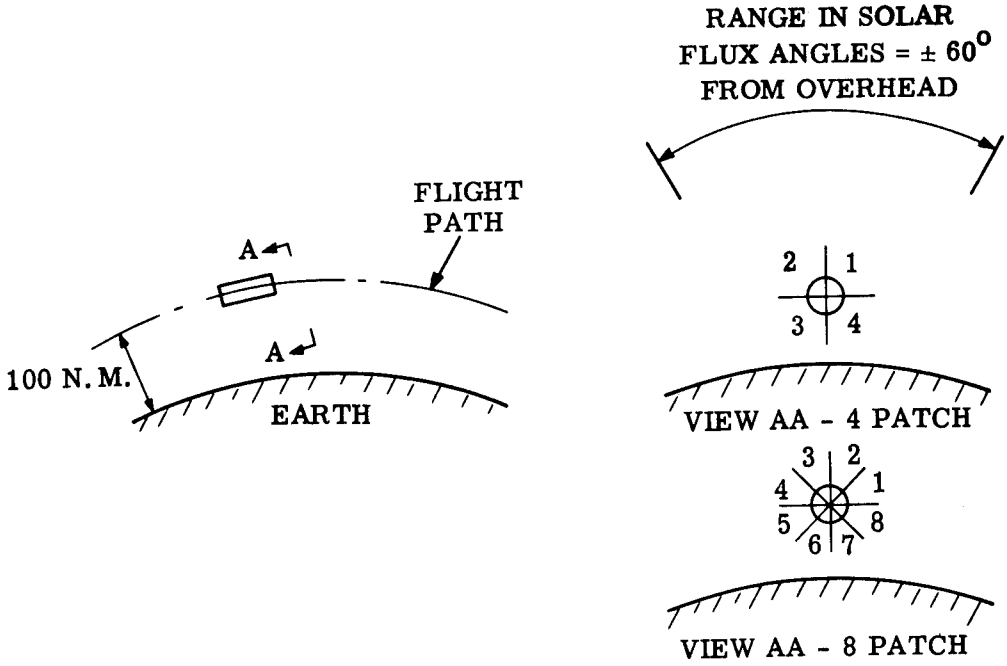

Figure 6. Orbit and Patch Geometry

TABLE III. ORBITAL HEAT FLUXES

Case	Patch	Orbit / Flux (BTU/hr ft^2)	1	2	3	4	5	6	7	8	9	10
1 Patch	1	(S+A)	107.7	90.4	79.5	90.4	107.7	91.1	70.7	59.9	70.7	91.1
		E	30.2	30.2	30.2	30.2	30.2	21.6	21.6	21.6	21.6	21.6
4 Patches	1	(S+A)	7.71	43.8	103.5	177.1	226.2	5.83	36.9	89.2	154.3	198.3
		E	6.36	6.36	6.36	6.36	6.36	4.54	4.54	4.54	4.54	4.54
	2	(S+A)	226.2	177.1	103.5	43.8	7.71	198.3	154.3	89.2	36.9	5.83
		E	6.36	6.36	6.36	6.36	6.36	4.54	4.54	4.54	4.54	4.54
	3	(S+A)	173.1	94.3	55.5	41.6	23.7	145.9	69.0	30.5	22.6	15.3
		E	53.4	53.4	53.4	53.4	53.4	38.6	38.6	38.6	38.6	38.6
	4	(S+A)	23.7	41.6	55.5	94.3	173.1	15.3	22.6	30.5	69.0	145.9
		E	53.4	53.4	53.4	53.4	53.4	38.6	38.6	38.6	38.6	38.6
8 Patches	1	(S+A)	5.54	9.62	68.3	187.3	288.8	2.99	5.19	46.4	161.7	252.5
		E	12.6	12.6	12.6	12.6	12.6	9.0	9.0	9.0	9.0	9.0
	2	(S+A)	9.85	77.9	138.6	166.9	163.6	8.67	68.6	122.1	147.0	144.1
		E	.117	.117	.117	.117	.117	.08	.08	.08	.08	.08
	3	(S+A)	163.6	166.8	138.6	77.9	9.85	144.1	147.0	122.1	68.6	8.67
		E	.117	.117	.117	.117	.117	.08	.08	.08	.08	.08
	4	(S+A)	288.8	187.3	68.3	9.62	5.58	252.5	161.7	56.4	5.19	2.98
		E	12.6	12.6	12.6	12.6	12.6	9.0	9.0	9.0	9.0	9.0
	5	(S+A)	254.9	116.2	43.7	30.8	17.8	221.5	91.9	22.1	16.6	12.7
		E	40.5	40.5	40.5	40.5	40.5	28.9	28.9	28.9	28.9	28.9
	6	(S+A)	91.4	72.4	67.3	52.4	29.7	70.4	46.2	39.0	28.6	16.0
		E	67.5	67.5	67.5	67.5	67.5	48.3	48.3	48.3	48.3	48.3
	7	(S+A)	29.7	52.4	67.3	72.4	91.4	16.0	28.6	39.0	46.2	70.4
		E	67.5	67.5	67.5	67.5	67.5	48.3	48.3	48.3	48.3	48.3
	8	(S+A)	17.8	30.8	43.7	116.2	254.9	12.7	16.6	22.1	91.9	221.5
		E	40.5	40.5	40.5	40.5	40.5	28.9	28.9	28.9	28.9	28.9

TABLE IV. RESULTS OF COATING-OPTIMIZATION STUDY

Specifications: Allowable α - ϵ Range: $0.1 \leq \epsilon \leq 0.9$, $0.1 \leq \alpha \leq 0.9$
Allowable Temperature Range:
Skin Temperatures: $200^{o}R$ to $800^{o}R$
Internal Temperature: $525^{o}R$ to $545^{o}R$

Results:

Node	Coating α	Coating ϵ	Temperature Range ^{o}R		
	Uniform Coating				
1 (External)	0.524	0.885	488.4	433.6	
2 (Internal)	-		552.5	517.5	(35^{o})
	4 Patches				
1	0.542	0.803	547.0	340.0	
2	0.544	0.796	548.5	340.4	
3	0.380	0.862	524.8	414.8	
4	0.381	0.863	524.8	414.8	
5 (Internal)	-		550.7	519.4	(31.7^{o})
	8 Patches				
1	0.362	0.862	529.8	342.6	
2	0.660	0.723	533.6	364.0	
3	0.652	0.727	531.9	363.9	
4	0.376	0.858	533.3	342.8	
5	0.314	0.878	527.2	388.8	
6	0.490	0.816	515.8	436.3	
7	0.492	0.814	516.3	436.4	
8	0.323	0.877	529.1	388.9	
9 (Internal)	-		546.0	523.1	(22.9^{o})

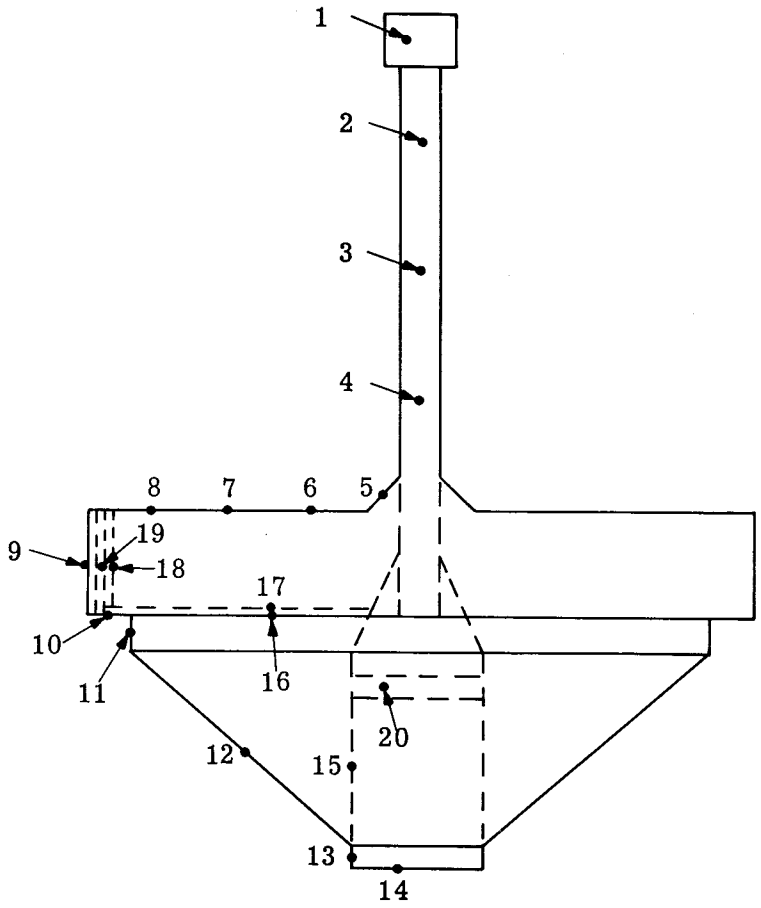

Figure 7. Nodal Breakdown for EPE-D

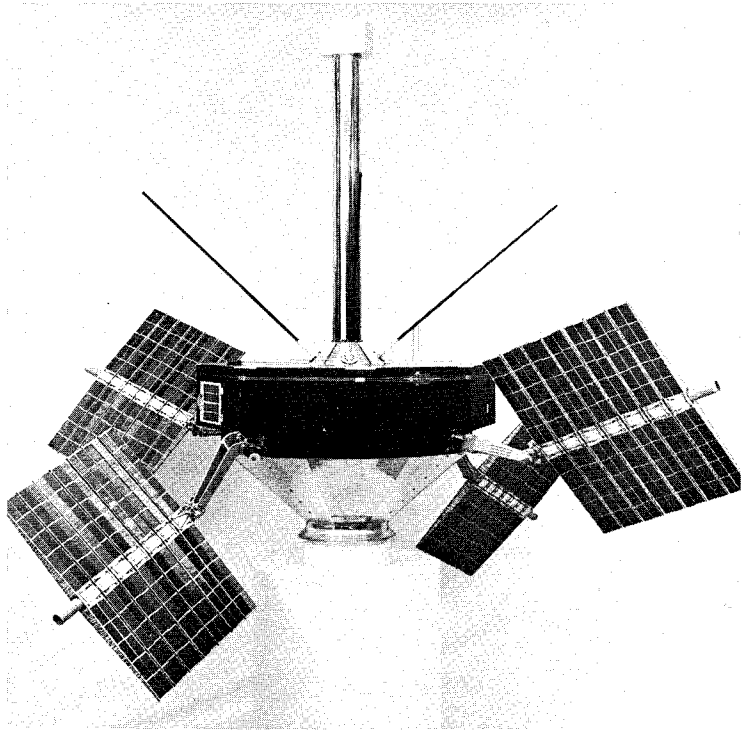

Figure 8. NASA's EPE-D (Explorer XXVI)

TABLE V: SUMMARY OF EPE-D DESIGNS

NODE	Temperature Ranges			
	Allowable Limits	Predicted Limits		
		Using NASA Coatings	Using Computer Solution	
			#1	#2	#3
1	420 - 564	468 - 537	438 - 489	478 - 542	411 - 492
6	456 - 600	471 - 600	482 - 578	477 - 572	432 - 618
7	456 - 600	468 - 599	478 - 583	475 - 574	434 - 624
8	456 - 600	470 - 578	479 - 566	482 - 566	443 - 611
17	492 - 546	495 - 535	496 - 539	499 - 540	486 - 538
18	492 - 546	509 - 524	510 - 529	501 - 540	493 - 524
20	474 - 582	488 - 564	497 - 574	517 - 572	456 - 580

NODE	Allowable Limits	Coatings Used							
		By NASA		Using Computer Solution					
				#1		#2		#3	
		α	ϵ	α	ϵ	α	ϵ	α	ϵ
1		.278	.260	.350	.849	.152	.118	.97	.86
2		.170	.112	.121	.032	.149	.115	.391	.826
3		.170	.112	.121	.034	.153	.116	.424	.81
4		.170	.112	.123	.038	.155	.118	.474	.776
5		.320	.260	.129	.040	.150	.119	.510	.768
6		.310	.240	.236	.232	.167	.196	.561	.457
7	Point 1: α=0.12 ϵ=0.03	.310	.240	.254	.20	.168	.199	.556	.560
8	Point 2: α=0.36 ϵ=0.26	.310	.240	.256	.179	.168	.198	.679	.574
9	Point 3: α=0.97 ϵ=0.86	.970	.850	.946	.853	.207	.166	.902	.793
10	Point 4: α=0.35 ϵ=0.85	.970	.850	.944	.859	.146	.123	.365	.667
11		.970	.850	.941	.859	.170	.147	.75	.644
12		.160	.110	.143	.108	.163	.183	.705	.599
13		.310	.240	.123	.039	.153	.123	.431	.792
14		.350	.850	.123	.039	.144	.116	.359	.764

NOTES:

1. Computer solutions differed only in their starting points, which were as follows:

   Case
   1 α=0.35, ϵ=0.85 for node 1; α=0.97, ϵ=0.86 for nodes 9, 10, 11; α=0.12, ϵ=0.03 for all other nodes.
   2 ϵ=α=0.12 for all nodes
   3 α=0.97, ϵ=0.86 for node 1; α=0.35, ϵ=0.85 for all other nodes

2. The third computer case terminated without attaining an acceptable solution. It appears that if the step size had not been reduced so rapidly, a better solution would have been attained.

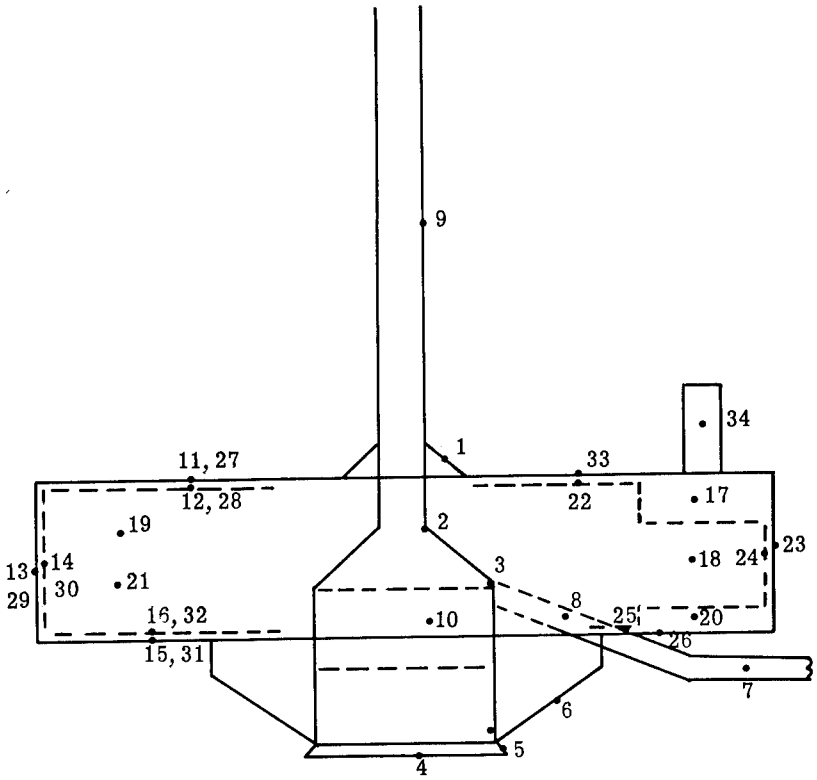

Figure 9. Nodal Breakdown For IMP-C

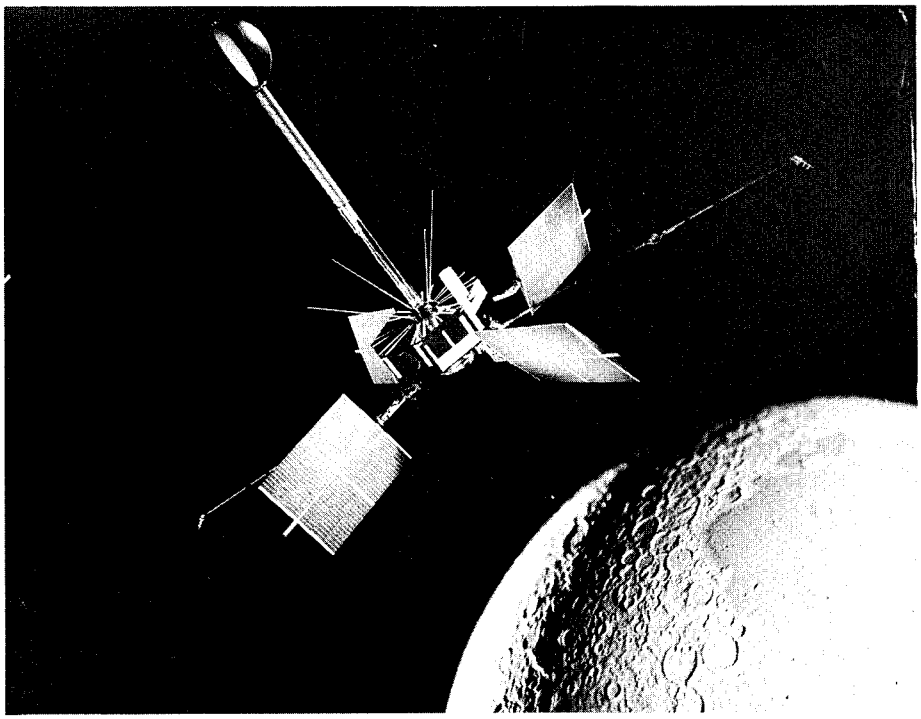

Figure 10. NASA's IMP-C

TABLE VI: SUMMARY OF IMP-C DESIGN

NODE	Temperature Ranges					
	Allowable Limits		Predicted Limits			
			Using NASA Coatings		Using Computer Solution	
2	501	555	499	539	504	545
3	501	555	483	532	505	529
4	492	555	474	526	496	539
10	501	555	492	532	505	534
17	474	600	528	591	515	592
18	492	555	503	530	505	530
19	501	555	503	553	504	535
20	474	564	537	578	538	560
21	501	555	496	537	504	537

NODE	Allowable Limits	Coatings Used			
		By NASA		Using Computer Solution	
		α	ϵ	α	ϵ
1		.17	.03	.613	.48
4		.25	.85	.12	.03
5		1.0	.84	.628	.496
6	ϵ = .03 ϵ = .04 ϵ = .86 ϵ = .85	.18	.188	.486	.387
7		.35	.84	.299	.704
9		.21	.03	.504	.364
11		.22	.188	.247	.786
13		.7	.81	.591	.670
15		.256	.24	.181	.415
23		.74	.82	.724	.598
25		.279	.636	.244	.815
27	α = .12 α = .2 α = .97 α = .25	.22	.188	.149	.218
29		.87	.82	.745	.621
31		.256	.157	.133	.111
33		.32	.188	.188	.459
34		.35	.84	.435	.718

7.0 CONCLUSIONS

The theoretical foundation and a detailed logic diagram have been developed from which a digital computer program has been devised that will select a space-vehicle external-coating pattern in such a way that the internal temperatures of the vehicle can be maintained as constant as possible in a purely passive manner.

The program has been demonstrated on several vehicle designs, three of which are shown in Section 6.0 of this report. It is seen that the gain of using a multiple-patch-external coating amounts to a factor of 2 in temperature variations from orbit to orbit. The coating pattern is derived in a direct method in a few minutes time on a digital computer with approximately 2-microsecond access time (such as an IBM 7094). The added expense of the enhanced design is seen to be quite small.

The details of the program will be found in Part II: User's Manual and Program Description.

8.0 RECOMMENDATIONS FOR FURTHER WORK

Time-Dependent Solutions

The present work assumes that the critical temperatures can be calculated using average heat fluxes, that is, that the component temperature deviates little from the average temperature. This assumption is good if the node heat capacitance is high compared to the equivalent thermal conductance between the node and its environment so that the time constant

$$\tau_{ci} \equiv \frac{(WC_p)_i}{L_{ii}} \tag{8.1}$$

(see Equation 3.4) is much greater than the time interval, τ, for which the average heat fluxes are calculated. If τ_{ci} is much greater than one orbit period, no difficulties arise.

For thin external surfaces, τ_{ci} is usually quite small, so that temperature deviations from the mean are large. It is therefore important to determine the true average temperatures and the magnitude of the deviation from the mean.

For transient heat flow, Equation (3.2) becomes

$$(WC_p)_i \frac{dT_i}{d\theta} + \sum_j \overline{A}_{ij} T_j + \sum_j M_{ij} T_j^4 = D_i(\theta) - \epsilon_i a_i \sigma T_i^4 \tag{8.2}$$

where

$$D_i(\theta) = \alpha_i S_i + \epsilon_i E_i + Q_i$$

Defining $\overline{X} = \frac{1}{\theta_1 - \theta_o} \int_{\theta_o}^{\theta_1} X \, d\theta$, integration of Equation (8.2) gives

$$(WC_p)_i \left[T_i(\theta_1) - T_i(\theta_o) \right] + \sum_j \overline{A}_{ij} \overline{T}_j + \sum_j M_{ij} \overline{T}_j^4 = \overline{D}_i - \epsilon_i a_i \sigma \overline{T}_i^4$$

If the temperature history is periodic of period τ_P, then, if $\theta_1 = \theta_o + \tau_P$, the heat-capacitance term is zero. If, in addition, $\overline{A}_{ij} \equiv 0$, the average fluxes will give the true average T^4's. If $\overline{A}_{ij} \neq 0$, then, since

$$\overline{T^4} \neq \overline{T}^4$$

neither the true average T^4 nor T are calculated. This is a problem that should be considered in future work. One approach would be to devise form factors, $\tilde{\gamma}$, such that

$$\overline{T^4} = \tilde{\gamma}\ \overline{T}^4$$

However, the development of this concept is beyond the scope of the present work.

Convergence of Iterative Solution

The heat-balance equation was solved for several numerical examples using seven iterative schemes. The fastest of the methods was then selected for the CSP. The rates of convergence should be investigated and compared on a more mathematical and rigorous basis.

Sub-optimizations of each iteration scheme should also be conducted. For example, one could determine if X could be made smaller for iteration schemes (1) and (2) (Table I), or one might add X to the L matrix of method (7) to determine if this aids convergence in such cases as Problem D (Table II).

"Typical" Orbits

In selecting the orbits used to obtain the optimum coating pattern, the usual approach is to take the extremes in, say, β-angles (i. e., the angle between solar ray and orbit plane), and then take a "few" orbits in between. This would give representative orbits for a uniformly coated vehicle. However, when the coating pattern is optimized for the particular orbits given in the input, it becomes questionable whether the particular orbits still represent extreme cases.

For most spacecraft, the environmental heat fluxes can be expressed as a function of one or two variables (β-angle, solar view-angle, orbit position, etc.), so a solution to the problem of properly selecting the orbits should be attainable.

Program Enlargement

The program is now limited to 34 nodes. For many satellites this is not adequate. The program can be enlarged if a LINK (chain) procedure is used, so that tape and drum storage is used.

Tolerances

The present program uses the nominal values of α and ϵ. The effects of tolerances in these values on the space vehicle temperatures must be calculated separately. This extra calculation could be incorporated in the optimization program.

Heaters and Shutters

The present program considers only those vehicles in which no auxiliary temperature control device is used. As such, it determines the best control that can be attained without such devices. The next step in determining the optimum temperature control system would be to include heaters and shutters (sometimes called louvres, vanes, or variable-surface-property devices).

9.0 APPENDICES

Appendix A. Mathematical Analysis of the TREND Step

The mathematical basis for TREND can be stated as follows:

Given two intersecting hypersurfaces, A and B. Given also a point 'a' on A and a point 'b' on B. 'b' lies on the projection of the maximum-rate-of-descent line of A through 'a', the projection being taken on the hyperplane $A(x_i) = 0$. The projected distance from 'a' to 'b' is 'Δs'. Given also a point 'c' on A having the same relationship to 'b' as 'b' does to 'a'.

We wish to prove that $A(\bar{c}) \leq A(\bar{a})$. If this is the case, then $B(d) \leq B(b)$, where 'd' is found using the maximum-rate-of-descent line from c. This process can be continued until a minimum value of A or B is reached. This will prove that the maximum-rate-of-descent method will converge to the minimum. For TREND, we must show also that $A(e) \leq A(c)$, where $\bar{e} - \bar{c} = [(\bar{c} - \bar{a})/|\bar{c} - \bar{a}|]\,\Delta s$.

Consider first the maximum rate of descent. The point b is given by

$$b_i = a_i - \frac{A_{xi}(\Delta s)}{\sqrt{\sum_i (A_{xi})^2}}$$

where the independent variables are taken as x_i. Also

$$c_i = b_i = - \frac{B_{xi}(\Delta s)}{\sqrt{\sum_i (B_{xi})^2}}$$

Therefore

$$c_i - a_i = -\left[\frac{A_{xi}}{\sqrt{\sum_i (A_{xi})^2}} + \frac{B_{xi}}{\sqrt{\sum_i (B_{xi})^2}}\right] \Delta s$$

Now

$$A(\bar{c}) = A(\bar{a}) + \sum_i A_{xi}(\bar{a}) \cdot (c_i - a_i) + \ldots$$

$$\doteq A(\bar{a}) - \sum_i \left[\frac{A_{xi}^2}{\sqrt{\sum A_{xi}^2}} + \frac{A_{xi}B_{xi}}{\sqrt{B_{xi}^2}}\right] \Delta s$$

Therefore

$$A(\bar{c}) \leq A(\bar{a}) \Longleftrightarrow \sqrt{\sum A_{xi}^2} \sum_i \left[\frac{A_{xi}^2}{\sqrt{\sum A_{xi}^2}} + \frac{A_{xi} B_{xi}}{\sqrt{\sum B_{xi}^2}} \right] \geq 0$$

Now $\sqrt{\sum A_{xi}^2} \geq 0$ and $\dfrac{A_{xi}}{\sqrt{\sum A_{xi}^2}}$ is the ith component of a unit vector from 'a', say

$$\bar{U}_1 = \sum_i \frac{A_{xi}}{\sqrt{\sum A_{xi}^2}} \bar{e}_i$$

Similarly

$$\bar{U}_2 = \sum_i \frac{B_{xi}}{\sqrt{\sum B_{xi}^2}} \bar{e}_i$$

Now

$$\bar{U}_1 \cdot \bar{U}_1 = 1$$

$$\bar{U}_1 \cdot \bar{U}_2 = \cos\theta$$

where θ is the angle between U_1 and U_2. Therefore

$$\bar{U}_1 \cdot \bar{U}_1 + \bar{U}_1 \cdot \bar{U}_2 = 1 + \cos\theta \geq 0$$

or

$$\sum_i \left[\frac{A_{xi}^2}{\left(\sqrt{\sum A_{xi}^2}\right)^2} + \frac{A_{xi} B_{xi}}{\sqrt{\left(\sum A_{xi}^2 \sum B_{xi}^2\right)}} \right] = 1 + \cos\theta \geq \theta$$

Therefore A(c) $\geq$ A(a), provided Δs is small enough that the first term of the Taylor's expansion is representative of the function A (no more than say 1/2% in error). If the radius for which the single term expansion is adequate, is designated R, it is required that $|\bar{c} - \bar{a}| \leq R$, or

$$\sum_i (c_i - a_i)^2 = \sum_i \left(\frac{A_{xi}}{\sqrt{\sum A_{xi}^2}} + \frac{B_{xi}}{\sqrt{\sum B_{xi}^2}} \right)^2 (\Delta s)^2 \leq R^2 \qquad \text{(A-1)}$$

The maximum value of the term inside the brackets is 4, so it is sufficient if

$$\Delta s \leq \frac{R}{2} = 0.5R \qquad \text{(A-2)}$$

In TREND, we wish to state also that $A(\bar{e}) \leq A(\bar{c})$, where

$$e_i - c_i = \frac{(c_i - a_i)}{\sqrt{\sum (c_i - a_i)^2}} (\Delta s)$$

Now if (Δs) is chosen small enough

$$A(\bar{e}) = A(\bar{a}) + \sum A_{xi}(\bar{a}) (e_i - a_i) + \ldots$$

$$\doteq A(\bar{a}) + \left[1 + \frac{\Delta s}{\sqrt{\sum (c_i - a_i)^2}} \right] \sum_i A_{xi}(\bar{a}) (c_i - a_i)$$

since

$$e_i - a_i = e_i - c_i + c_i - a_i = (c_i - a_i) \left(\frac{e_i - c_i}{c_i - a_i} + 1 \right)$$

Therefore

$$A(\bar{e}) - A(\bar{c}) = \frac{\Delta s}{\sqrt{\sum_i (c_i - a_i)^2}} \sum_i A_{xi}(\bar{a}) (c_i - a_i)$$

$$= \frac{\Delta s}{\sqrt{\sum_i (c_i - a_i)^2}} \left[A(\bar{c}) - A(\bar{a}) \right] \leq 0$$

which proves the validity of TREND. The (Δs) must be chosen such that

$$\left| \bar{e} - \bar{a} \right| \leq R$$

or

$$\sum_i (e_i - a_i)^2 \leq R^2$$

or

$$\left[1 + \frac{\Delta s}{\sqrt{\sum (c_i - a_i)^2}}\right]^2 \sum_i (c_i - a_i)^2 \leq R^2$$

but

$$\sum_i (c_i - a_i)^2 \leq 4 (\Delta s)^2 \qquad \text{From Equation (A-1)}$$

$$\therefore \sum_i (c_i - a_i)^2 + 2(\Delta s) \sqrt{\sum (c_i - a_i)^2} + (\Delta s)^2 \leq 4(\Delta s)^2 + 4(\Delta s)^2 + (\Delta s)^2 = 9 (\Delta s)^2$$

Therefore, Δs must be such that

$$\Delta s \leq \frac{1}{3} R = 0.333R \qquad \text{(A-3)}$$

It is seen by comparison between Equations (A-2) and (A-3) that TREND will be slower than MRD if the A_{xi}'s equal the B_{xi}'s; that is, if the two steps of MRD are approximately in the same direction. However, if $c_i \doteq a_i$, so that $\Sigma(c_i - a_i)^2 = \epsilon^2$, MRD will move with net step sizes on A of ϵ and convergence will be slow. TREND, under the same circumstances will proceed with a net step size of $(\epsilon + \Delta s)$.

Appendix B. Convergence of the Inverse-Matrix Iteration Methods

To analyze the convergence of the matrix inversion iteration schemes (Methods 1 and 2 of Table I), it is necessary to linearize the radiation terms. Let

$$\bar{R}_{ij} = \begin{cases} -\sigma R_{ij} (\tilde{T}_i + \tilde{T}_j)(\tilde{T}_i^2 + \tilde{T}_j^2) & i \neq j \\ -\sum_{\substack{j=1 \\ j\neq i}}^{N+S} \bar{R}_{ij} + 4 a_i \epsilon_i \sigma \tilde{T}_i^3 \end{cases} \tag{B-1}$$

Then Equation (3.2) becomes

$$\sum_{j=1}^{N+S} (\bar{A}_{ij} + \bar{R}_{ij}) T_j = C_i$$

where C_i is defined as in Equation (3.4).

Method (1) solves this equation in the form

$$T^{(n+1)} = (\bar{A} + X)^{-1} (C - (\bar{R} - X) T^{(n)}) \tag{B-2}$$

Convergence of the iteration process depends, then, on the spectral radius, $\rho(Z)$, of

$$Z \equiv (\bar{A} + X)^{-1} (X - \bar{R}) \tag{B-3}$$

being less than one.

Note that

$$\left.\begin{aligned} (\bar{A} + X)_{ii} &\geq -\sum_{j=1}^{N} \bar{A}_{ij} \quad \text{and} \quad \bar{A}_{ij} \leq 0 \quad i \neq j \\ \bar{R}_{ii} &\geq -\sum_{j=1}^{N} \bar{R}_{ij} \quad \text{and} \quad \bar{R}_{ij} \leq 0 \quad i \neq j \\ X_{ii} &\geq 0 \quad \text{and} \quad X_{ij} = 0 \quad i \neq j \end{aligned}\right\} \tag{B-4}$$

The matrix $(\bar{A} + X)^{-1}$ is positive by virtue of Equations (B-4). If, in addition $X_{ii} \geq \bar{R}_{ii}$, $(X - \bar{R})$ is positive so that, since

$$(\bar{A} + \bar{R}) = (\bar{A} + X) - (X - \bar{R}) \quad \text{with} \quad (\bar{A} + \bar{R})^{-1} \geq 0, \tag{B-5}$$

$\left[(\bar{A} + X) - (X - \bar{R})\right]$ is a regular splitting of the matrix $(\bar{A} + \bar{R})$. Then by Theorem 2.2 of Varga[6]

$$\rho(Z) = \frac{\rho\left[(\bar{A} + \bar{R})^{-1} (X - R)\right]}{1 + \rho\left[(\bar{A} + \bar{R})^{-1} (X - R)\right]} < 1 \tag{B-6}$$

so that convergence is assured if $X_{ii} = \bar{R}_{ii}$. By Theorem 2.7 of Varga, it is evident that $X_{ii} = \bar{R}_{ii}$ gives the minimum value of ρ (Z) and, therefore, the most rapid convergence.

Relating the foregoing to the non-linear equation shows that a sufficient condition for convergence is that

$$X_{ii} \geq - \sum_{\substack{j=i \\ j\neq i}}^{N+S} \sigma R_{ij} (T_i + T_j)_{max} (T_i^2 + T_j^2)_{max} + 4 a_i \epsilon_i \sigma T_{i\,max}^3 \qquad \text{(B-7)}$$

and that most rapid convergence will occur if

$$X_{ii} = - \sum_{\substack{j=i \\ j\neq i}}^{N+S} \sigma R_{ij} (T_i + T_j) (T_i^2 + T_j^2) + 4 a_i \epsilon_i \sigma T_i^3 \qquad \text{(B-8)}$$

where T_k and X_{ii} are evaluated at each iteration. This latter criteria can be approximated by using T_i as T_j, solution.

It is evident that if Equation (B-8) is satisfied, Equation (B-7) will, in general, be violated. Although it has not been shown in a mathematically rigorous fashion, experience with many numerical cases indicates that the criteria expressed in Equation (B-7) can be relaxed somewhat so that convergence will occur if

$$X_{ii} = \max \left[\frac{1}{2} (\bar{R}_{ii}^* - A_{ii}); \sum_{j\neq i} \left| \bar{A}_{ij} \right| - \bar{A}_{ii}; \sum_{j\neq i} (-\bar{R}_{ij}^* + \bar{A}_{ij}) - \bar{A}_{ii} \right] \qquad \text{(B-9)}$$

where $\bar{R}_{ij}^* = \bar{R}_{ij}$ evaluated with T_i and T_j at their maximum anticipated values.

Combining Equations (B-8) and (B-9) gives the following criteria on X_{ii}:

$$X_{ii} = \max \left[\frac{1}{2} (\bar{R}_{ii}^* - \bar{A}_{ii}); \sum_{j\neq i} \left| \bar{A}_{ij} \right| - \bar{A}_{ii}; \sum_{j\neq i} (-\bar{R}_{ij}^* + \bar{A}_{ij}) - \bar{A}_{ii}; \bar{R}_{ii}^o \right] \qquad \text{(B-10)}$$

(Method 1)

where $\bar{R}_{ii}^o = \bar{R}_{ii}$ evaluated with T_i and T_j at their anticipated solution values.

The analysis of Method (2) follows the same pattern as for Method (1). The counterpart of Equation (B-10) is found by replacing $\bar{R}$ in Equation (B-10) by $\bar{R} - \bar{R}^o$.

$$X_{ii} = \max \left[\frac{1}{2} (\bar{R}_{ii}^* - \bar{R}_{ii}^o - \bar{A}_{ii}); \sum_{j\neq i} \left| \bar{A}_{ij} \right| - \bar{A}_{ii}; \sum_{j\neq i} (-\bar{R}_{ij}^* + \bar{R}_{ij}^o + \bar{A}_{ij}) - \bar{A}_{ii}; 0 \right] \qquad \text{(B-11)}$$

(Method 2)

LOGIC DIAGRAM FOR TREND

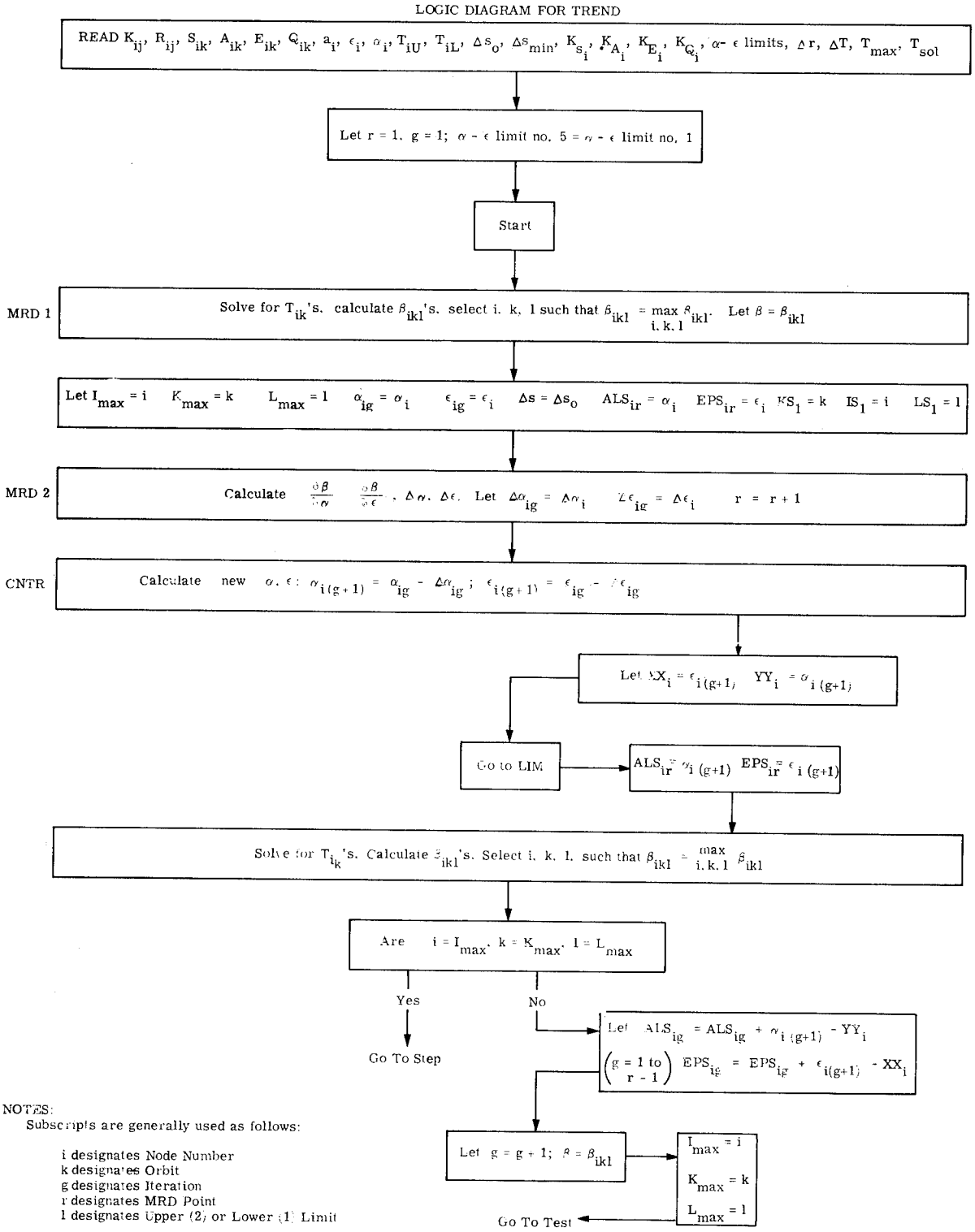

NOTES:
Subscripts are generally used as follows:

i designates Node Number
k designates Orbit
g designates Iteration
r designates MRD Point
l designates Upper (2) or Lower (1) Limit

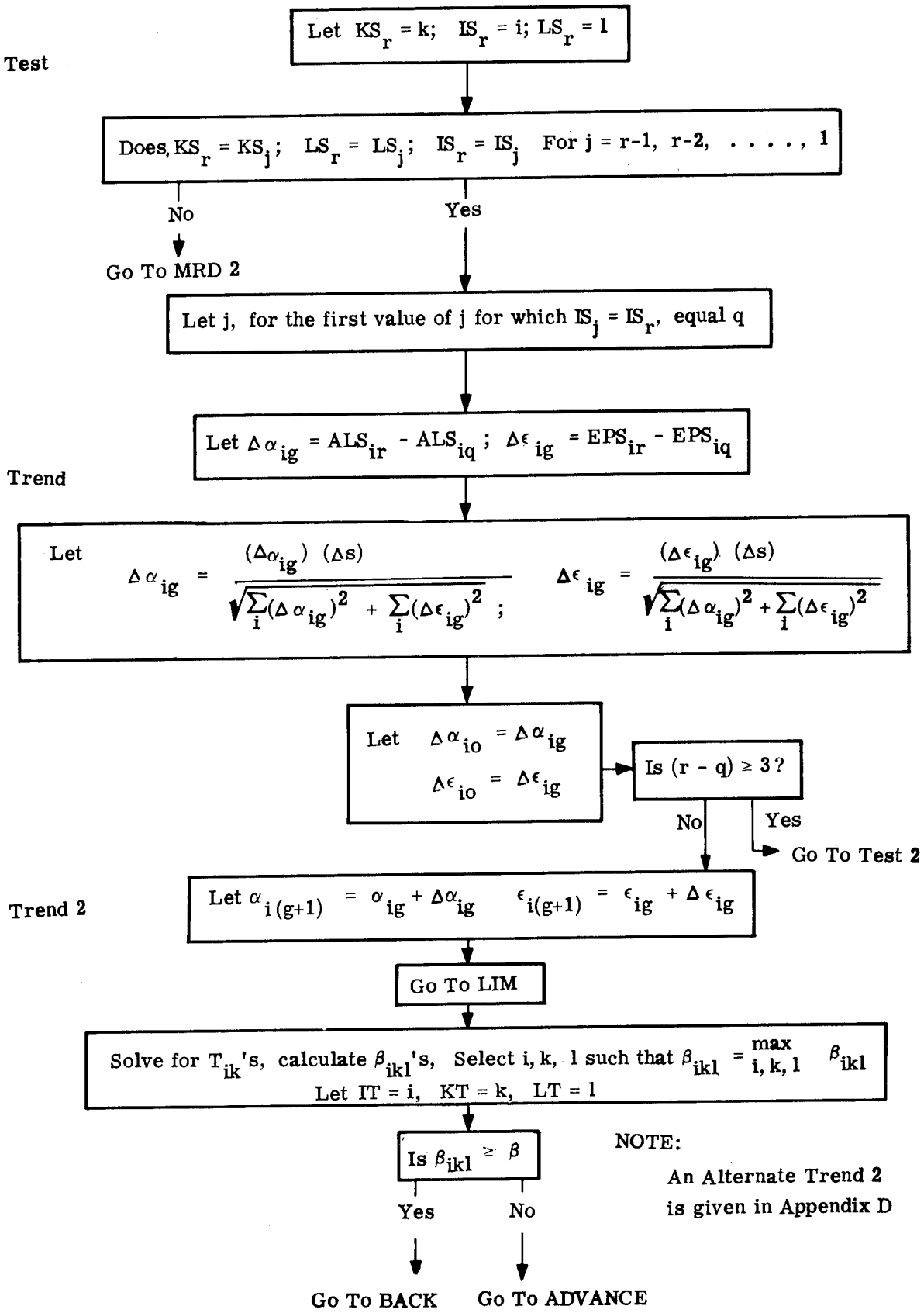
Test
Let $KS_r = k$; $IS_r = i$; $LS_r = 1$
Does, $KS_r = KS_j$; $LS_r = LS_j$; $IS_r = IS_j$ For j = r-1, r-2, ... , 1
No
Yes
Go To MRD 2
Let j, for the first value of j for which $IS_j = IS_r$, equal q
Trend
Let $\Delta\alpha_{ig} = ALS_{ir} - ALS_{iq}$; $\Delta\epsilon_{ig} = EPS_{ir} - EPS_{iq}$
Let $\Delta\alpha_{ig} = \frac{(\Delta\alpha_{ig})\ (\Delta s)}{\sqrt{\sum_i (\Delta\alpha_{ig})^2 + \sum_i (\Delta\epsilon_{ig})^2}}$; $\Delta\epsilon_{ig} = \frac{(\Delta\epsilon_{ig})\ (\Delta s)}{\sqrt{\sum_i (\Delta\alpha_{ig})^2 + \sum_i (\Delta\epsilon_{ig})^2}}$
Let $\Delta\alpha_{io} = \Delta\alpha_{ig}$
$\Delta\epsilon_{io} = \Delta\epsilon_{ig}$
Is (r - q) ≥ 3?
No
Yes
Go To Test 2
Trend 2
Let $\alpha_{i(g+1)} = \alpha_{ig} + \Delta\alpha_{ig}$ $\epsilon_{i(g+1)} = \epsilon_{ig} + \Delta\epsilon_{ig}$
Go To LIM
Solve for T_{ik}'s, calculate β_{ikl}'s, Select i, k, l such that $\beta_{ikl} = \max_{i,k,l} \beta_{ikl}$
Let IT = i, KT = k, LT = l
Is $\beta_{ikl} \geq \beta$
Yes
No
Go To BACK
Go To ADVANCE
NOTE:
An Alternate Trend 2
is given in Appendix D

STEP

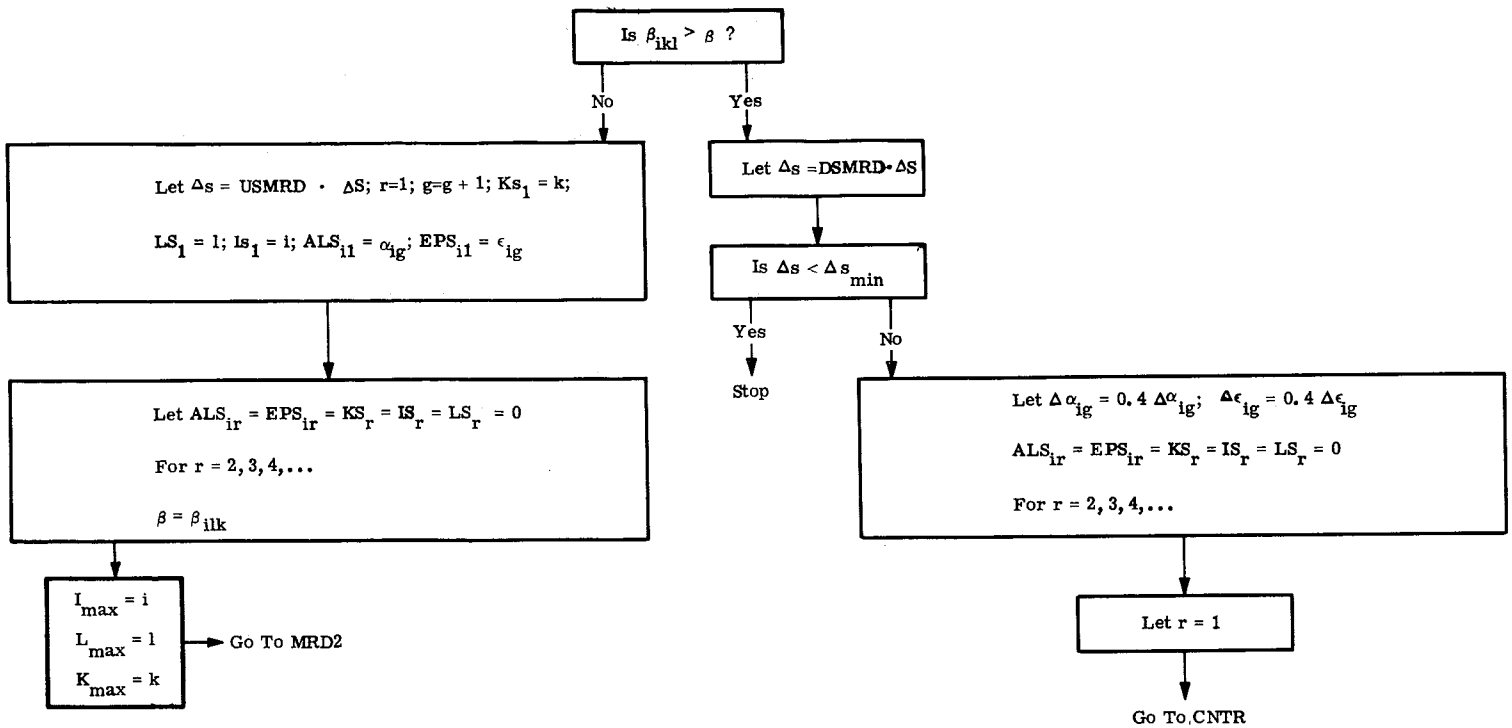

ADVANCE

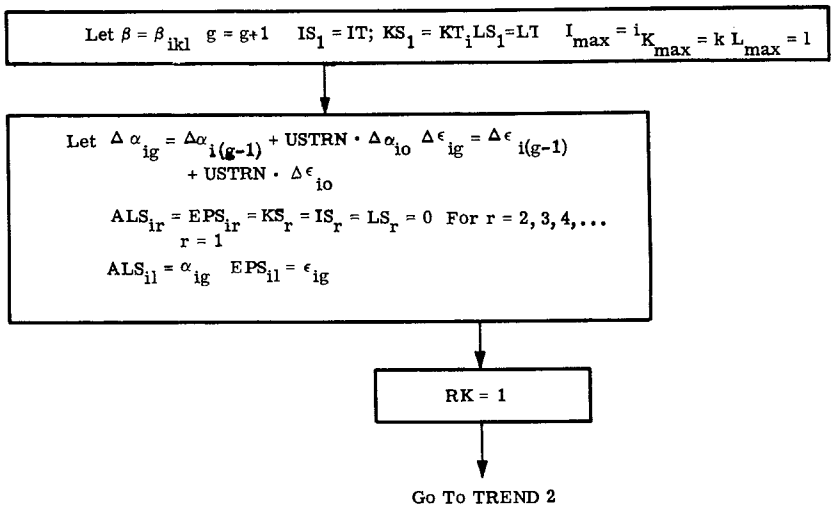

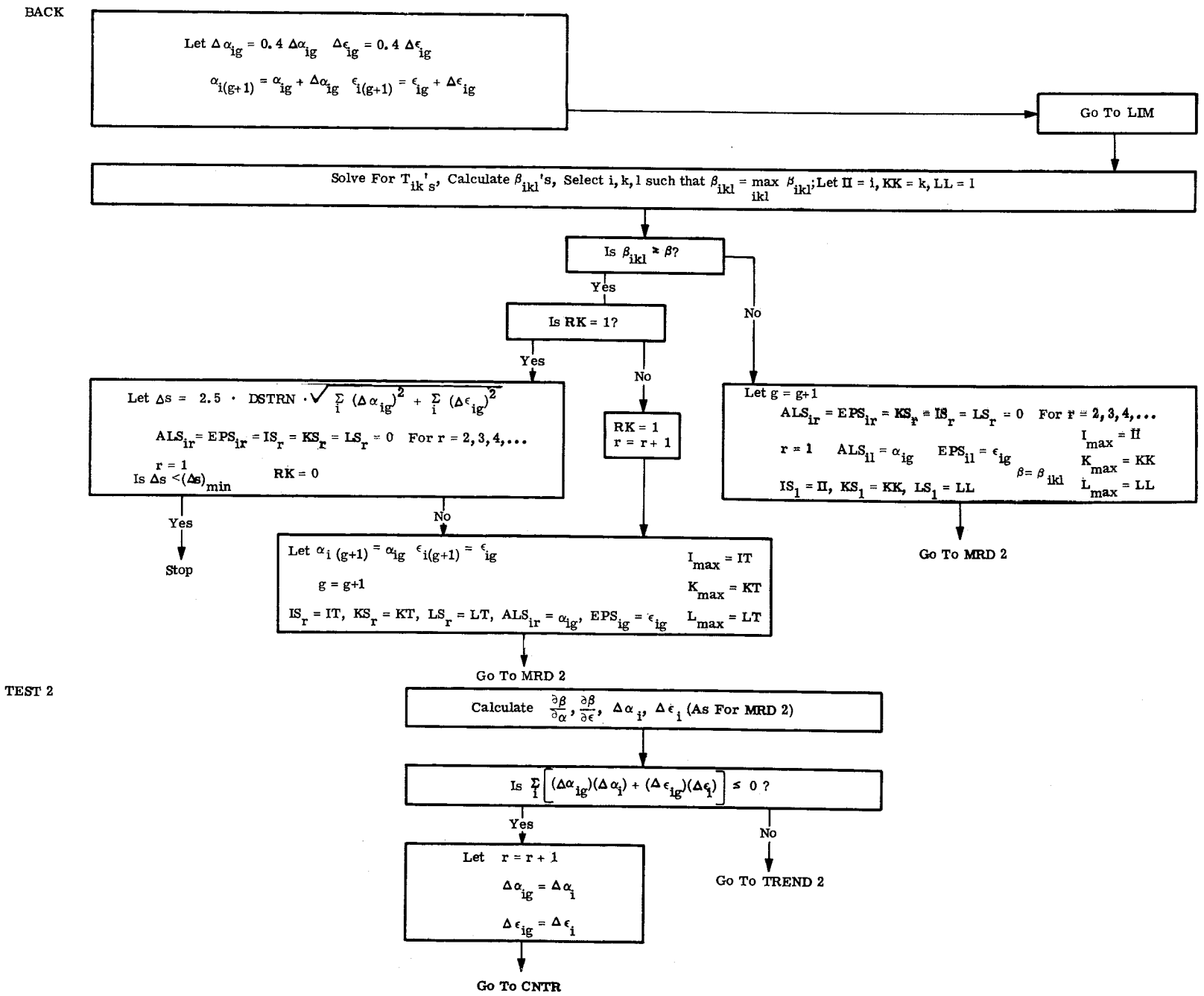
BACK
Let $\Delta\alpha_{ig} = 0.4\ \Delta\alpha_{ig}$ $\Delta\epsilon_{ig} = 0.4\ \Delta\epsilon_{ig}$
$\alpha_{i(g+1)} = \alpha_{ig} + \Delta\alpha_{ig}$ $\epsilon_{i(g+1)} = \epsilon_{ig} + \Delta\epsilon_{ig}$
Go To LIM
Solve For T_{ik}'s, Calculate β_{ikl}'s, Select i, k, l such that $\beta_{ikl} = \max_{ikl} \beta_{ikl}$; Let II = i, KK = k, LL = l
Is $\beta_{ikl} \geq \beta$?
Yes
No
Is RK = 1?
Yes
No
Let $\Delta s = 2.5 \cdot DSTRN \cdot \sqrt{\sum_i (\Delta\alpha_{ig})^2 + \sum_i (\Delta\epsilon_{ig})^2}$
$ALS_{ir} = EPS_{ir} = IS_r = KS_r = LS_r = 0$ For r = 2, 3, 4, ...
r = 1
Is $\Delta s < (\Delta s)_{min}$
RK = 0
RK = 1
r = r + 1
Let g = g+1
$ALS_{ir} = EPS_{ir} = KS_r = IS_r = LS_r = 0$ For r = 2, 3, 4, ...
r = 1 $ALS_{il} = \alpha_{ig}$ $EPS_{il} = \epsilon_{ig}$
$IS_1 = II$, $KS_1 = KK$, $LS_1 = LL$
$\beta = \beta_{ikl}$
$I_{max} = II$
$K_{max} = KK$
$L_{max} = LL$
Yes
No
Stop
Let $\alpha_{i(g+1)} = \alpha_{ig}$ $\epsilon_{i(g+1)} = \epsilon_{ig}$
g = g+1
$IS_r = IT$, $KS_r = KT$, $LS_r = LT$, $ALS_{ir} = \alpha_{ig}$, $EPS_{ig} = \epsilon_{ig}$
$I_{max} = IT$
$K_{max} = KT$
$L_{max} = LT$
Go To MRD 2
Go To MRD 2
TEST 2
Calculate $\frac{\partial\beta}{\partial\alpha}$, $\frac{\partial\beta}{\partial\epsilon}$, $\Delta\alpha_i$, $\Delta\epsilon_i$ (As For MRD 2)
Is $\sum_I \left[(\Delta\alpha_{ig})(\Delta\alpha_i) + (\Delta\epsilon_{ig})(\Delta\epsilon_i)\right] \leq 0$?
Yes
No
Let r = r + 1
$\Delta\alpha_{ig} = \Delta\alpha_i$
$\Delta\epsilon_{ig} = \Delta\epsilon_i$
Go To TREND 2
Go To CNTR

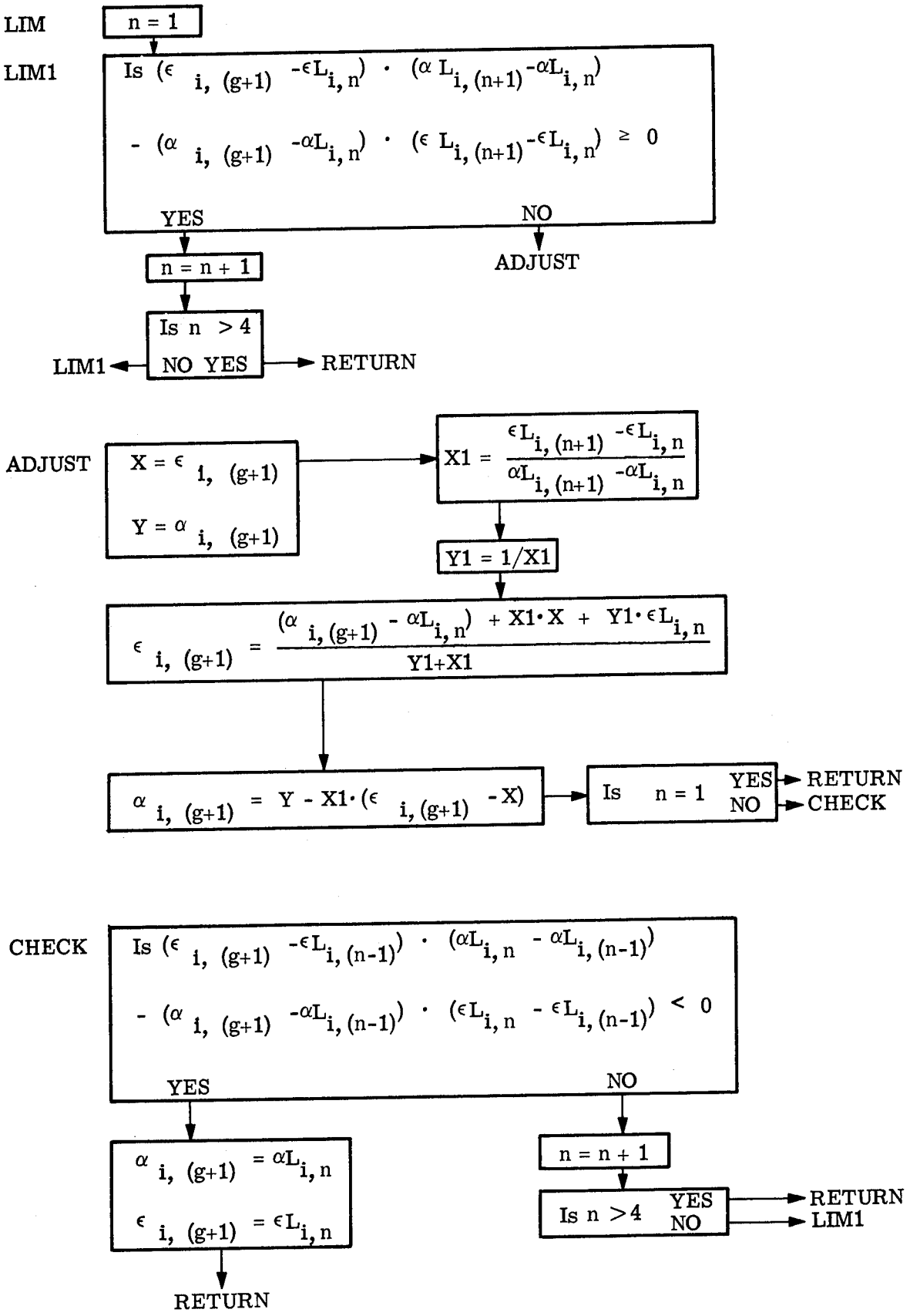
LIM
n = 1
LIM1
Is $(\epsilon_{i,(g+1)} - \epsilon L_{i,n}) \cdot (\alpha L_{i,(n+1)} - \alpha L_{i,n})$
$- (\alpha_{i,(g+1)} - \alpha L_{i,n}) \cdot (\epsilon L_{i,(n+1)} - \epsilon L_{i,n}) \geq 0$
YES
NO
ADJUST
n = n + 1
Is n > 4
NO YES
LIM1
RETURN
ADJUST
$X = \epsilon_{i,(g+1)}$
$Y = \alpha_{i,(g+1)}$
$X1 = \frac{\epsilon L_{i,(n+1)} - \epsilon L_{i,n}}{\alpha L_{i,(n+1)} - \alpha L_{i,n}}$
Y1 = 1/X1
$\epsilon_{i,(g+1)} = \frac{(\alpha_{i,(g+1)} - \alpha L_{i,n}) + X1 \cdot X + Y1 \cdot \epsilon L_{i,n}}{Y1+X1}$
$\alpha_{i,(g+1)} = Y - X1 \cdot (\epsilon_{i,(g+1)} - X)$
Is n = 1
YES
NO
RETURN
CHECK
CHECK
Is $(\epsilon_{i,(g+1)} - \epsilon L_{i,(n-1)}) \cdot (\alpha L_{i,n} - \alpha L_{i,(n-1)})$
$- (\alpha_{i,(g+1)} - \alpha L_{i,(n-1)}) \cdot (\epsilon L_{i,n} - \epsilon L_{i,(n-1)}) < 0$
YES
NO
$\alpha_{i,(g+1)} = \alpha L_{i,n}$
$\epsilon_{i,(g+1)} = \epsilon L_{i,n}$
RETURN
n = n + 1
Is n > 4
YES
NO
RETURN
LIM1

Appendix D. Nomenclature (Excepted and Noted)

Symbol	Description	Suggested Units
A	incident albedo flux	BTU/hr ft^2
$\bar{A}$	conduction matrix term	BTU/hr ^oF
C	defined by Equation (3.4)	BTU/hr
D	defined by Equation (8.2)	BTU/hr
E	incident earth flux	BTU/hr ft^2
$\tilde{E}_{ij}$	$(\partial r_i/\partial T_j)$ at $T_i = T_j^{(0)}$	BTU/hr ^oF
J	inverse matrix of $\bar{A}$	hr ^oF/BTU
K_{Ai}	multiplier of incident albedo flux for node 'i'	ft^2
K_{Ei}	multiplier of incident earth flux for node 'i'	ft^2
K_{Qi}	multiplier of internal heat generation	BTU/watt hr
K_{ij}	conductance from node 'i' to node 'j'	BTU/hr ^oF
K_{Si}	multiplier of incident solar flux for node 'i'	ft^2
L	defined by Equation (3.4)	BTU/hr ^oF
M	radiation-matrix term	BTU/hr ft^2 $(^oR)^4$
N	defined by Equation (4.3)	BTU/hr $(^oR)^4$
P	inverse of $N_{ij} + \epsilon_i \delta_{ij}$	hr $(^oR)^4$/BTU
Q	internal heat generation	watts
$\bar{R}$	defined by Equation (9.2.1)	BTU/hr ^oF
R_{ij}	product of radiant interchange factor between nodes 'i' and 'j' and area of node 'i'	ft^2
(RHS)	defined by Equation (4.10)	BTU/hr
S	incident solar flux	BTU/hr ft^2
T	absolute temperature	^oR
$(WC_p)_i$	heat capacitance of node 'i'	BTU/^oF
X	stability parameter in matrix inversion methods	BTU/hr ^oF

Symbol	Description	Suggested Units
Y	$\sigma a_i T_i^4 - K_{Ei} E_i$	BTU/hr
a_i	re-radiating area for node 'i' (external area)	ft^2
c	weighting factor, Equation (2.3)	-
d	weighting factor, Equation (2.4)	-
r	residual vector (Equation 3.5)	BTU/hr
α	solar absorptance	-
α_n	iteration scheme extrapolation parameter	-
β	temperature deviation parameter	-
γ	criterion function, Equations (2.3) and (2.4)	-
$\tilde{\gamma}$	form factor, $(\overline{T^4})/(\overline{T})^4$	-
δ_{ij}	Kronecker delta (=1 if i=j; =o if i≠j)	-
ϵ	infrared emittance	-
θ	time	hrs
λ	interpolation parameter	-
σ	Stephen-Boltzmann constant (0.1713×10^{-8})	BTU/hr ft^2 $(^oR)^4$
τ_{ci}	$(WC_p)_i/L_{ii}$	hrs
Subscripts		
i	usually node number	
iL	corresponding to lower limit on T_i	
iU	corresponding to upper limit on T_i	
k	usually orbit number	
Superscript		
n	iteration number	

10.0 REFERENCES

1. Linder, B., "Advanced Thermal Control Coatings", GE Report TIS 65SD4246, March 5, 1965.

2. Costello, F. A., Harper, T. P., and Cline, P. B., "A Rational Approach to the Selection of Satellite Optical Coating Patterns For Temperature Control", ASME Paper 63-HT-41, August, 1963.

3. Fox, L., An Introduction to Numercial Linear Algebra, Clarendon Press, Oxford (1964).

4. Kaplan, B. and Clark, N., "Accelerating the Convergence of the Generalized Transient Heat Transfer Program (THT)", GE-ANPD Report XDC-60-5-8 (March 31, 1960).

5. Hadley, G., Nonlinear and Dynamic Programming, Addison-Wesley Publishing Company, Inc. (1964).

6. Varga, S., "Matrix Iterative Analysis", Prentice-Hall, Inc. (1962).

"The aeronautical and space activities of the United States shall be conducted so as to contribute . . . to the expansion of human knowledge of phenomena in the atmosphere and space. The Administration shall provide for the widest practicable and appropriate dissemination of information concerning its activities and the results thereof."

—NATIONAL AERONAUTICS AND SPACE ACT OF 1958

NASA SCIENTIFIC AND TECHNICAL PUBLICATIONS

TECHNICAL REPORTS: Scientific and technical information considered important, complete, and a lasting contribution to existing knowledge.

TECHNICAL NOTES: Information less broad in scope but nevertheless of importance as a contribution to existing knowledge.

TECHNICAL MEMORANDUMS: Information receiving limited distribution because of preliminary data, security classification, or other reasons.

CONTRACTOR REPORTS: Scientific and technical information generated under a NASA contract or grant and considered an important contribution to existing knowledge.

TECHNICAL TRANSLATIONS: Information published in a foreign language considered to merit NASA distribution in English.

SPECIAL PUBLICATIONS: Information derived from or of value to NASA activities. Publications include conference proceedings, monographs, data compilations, handbooks, sourcebooks, and special bibliographies.

TECHNOLOGY UTILIZATION PUBLICATIONS: Information on technology used by NASA that may be of particular interest in commercial and other non-aerospace applications. Publications include Tech Briefs, Technology Utilization Reports and Notes, and Technology Surveys.

Details on the availability of these publications may be obtained from:

SCIENTIFIC AND TECHNICAL INFORMATION DIVISION

NATIONAL AERONAUTICS AND SPACE ADMINISTRATION

Washington, D.C. 20546